---

**Article:**
Yefremova, Y, Melder, FTI, Danquah, BD et al. (8 more authors) (2017) Apparent activation energies of protein–protein complex dissociation in the gas–phase determined by electrospray mass spectrometry. Analytical and Bioanalytical Chemistry, 409 (28). pp. 6549-6558. ISSN 1618-2642

https://doi.org/10.1007/s00216-017-0603-4

---

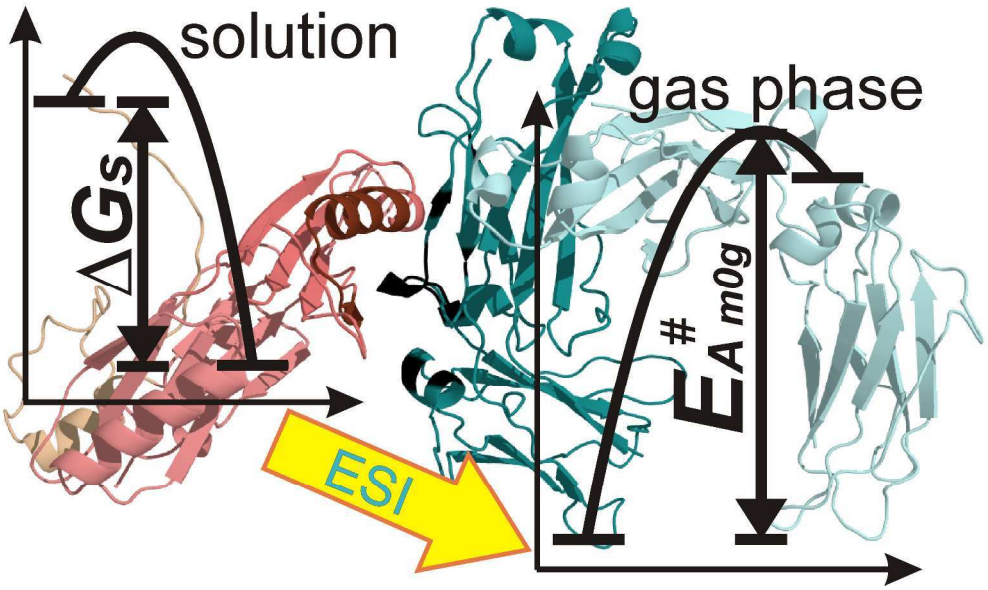


Graphical abstract

263x158mm (300 x 300 DPI)

# Apparent Activation Energies of Protein-Protein Complex Dissociation in the Gas Phase Determined by Electrospray Mass Spectrometry

Yelena Yefremova[1,¥], F. Teresa I. Melder[1,¥], Bright D. Danquah[1], Kwabena F.M. Opuni[1,#], Cornelia Koy[1], Alexandra Ehrens[2,+], David Frommholz[2], Harald Illges[2], Knut Koelbel[3], Frank Sobott[3,4,5], Michael O. Glocker[1,*]

1) Proteome Center Rostock, University Rostock Medical Center, Schillingallee 69, 18059 Rostock, Germany

2) University of Applied Sciences Bonn-Rhein-Sieg, Grantham-Allee 20, 53757 Bonn, Germany

3) University of Antwerp, Department of Chemistry, Groenenborgerlaan 171, 2020 Antwerp, Belgium

4) Astbury Centre for Structural Molecular Biology, University of Leeds, Leeds LS2 9JT, United Kingdom

5) School of Molecular and Cellular Biology, University of Leeds, Leeds LS2 9JT, UK

[#] present address: School of Pharmacy, University of Ghana, P.O. Box LG43, Legon Accra, Ghana

[+] present address: University Hospital of Bonn, Sigmung-Freud-Str. 25, 53105 Bonn, Germany

* Corresponding author, e-mail: michael.glocker@med.uni-rostock.de

[¥] Yelena Yefremova and F. Teresa I. Melder contributed equally to this work.

## Running title

Thermodynamics of protein-protein complex dissociation in the gas phase

## Abstract

We have developed a method to determine apparent activation energies of dissociation for ionized protein-protein complexes in the gas phase using electrospray ionization mass spectrometry following the Rice-Ramsperger-Kassel-Marcus quasi-equilibrium theory. Protein-protein complexes were formed in solution, transferred into the gas phase and separated from excess free protein by ion mobility filtering. Afterwards, complex disassembly was initiated by collision induced dissociation with step-wise increasing energies. Relative intensities of ion signals were used to calculate apparent activation energies of dissociation in the gas phase by applying linear free energy relations. The method was developed using streptavidin tetramers. Experimentally determined apparent gas phase activation energies for dissociation ($E^{\#}_{A\,m0g}$) of complexes consisting of Fc parts from immunoglobulins (IgG-Fc) and three closely related protein G´ variants (IgG-Fc•protein G´e, IgG-Fc•protein G´f, and IgG-Fc•protein G´g) show the same order of stabilities as can be inferred from their in-solution binding constants. Differences in stabilities between the protein-protein complexes correspond to single amino acid residue exchanges in the IgG-binding regions of the protein G´ variants.

## Key words

Protein-protein interaction, native mass spectrometry, ion mobility, collision induced dissociation, quasi equilibrium conditions

## Abbreviations

Protein G': protein G prime

Protein G'e: protein G prime e (extended)

Protein G'f: protein G prime f

Protein G'g: protein G prime g

IgG: immunoglobulin G

IVIG: intravenous immunoglobulin

Fc part: fragment crystallizable part

ESI: electrospray ionization

ToF: time of flight

$K_{D\,s}$: dissociation constant in solution

$\Delta G_s$: Gibbs free energy difference in solution

LFE: linear free energy

$E_{A\,m0g}^{\#}$: $E_A$: energy of activation, #: apparent (with merged temperature term), m: mean of charge states, 0: at $E_{com}$=0 eV, g: gas phase.

$K_{D\,m0g}^{\#}$: $K_D$: dissociation constant, #: apparent (with merged temperature term), m: mean of charge states, 0: at $E_{com}$=0 eV, g: gas phase.

## Introduction

Already in the mid-90s of the last century the possibility to characterize non-covalent bio-macromolecular complexes using electrospray mass spectrometry became evident [1,2]. More recent studies provided strong indications that upon transfer into the gas phase proteins retained compact conformations [3] that could be investigated by so-called "native ESI-MS" and ion mobility MS (IM-MS) [4-6]. These methods are now widely applied for determining qualitative properties of protein complexes, such as topology, size, subunit organization, and stoichiometry [7-9].

In solution, protein-protein interactions are characterized quantitatively by dissociation constants ($K_{D\,s}$) and Gibbs free binding energies ($\Delta G_S^0$) at equilibrium [10] which are typically determined using calorimetric or spectroscopic methods [11]. In some cases, mass spectrometry-based methods have been applied as read-outs for determining in-solution $K_D$ values of protein-protein complexes by comparing ion signal intensities of free and complexed proteins at different solution concentrations of the complex components [12-15]. Introducing correction factors for differences of surface activities of analytes in the droplet as well as for additional gas phase ion suppression effects [16] yielded satisfactory correlation with results from conventional methods.

There are, however, currently no universally accepted gas-phase equivalents to typical thermodynamic and/or kinetic methods for evaluating protein-protein complex properties. In one case, activation energies of thermal protein-protein complex dissociation in the gas phase were deduced by observing complex dissociation kinetics upon blackbody infrared radiation using Fourier-transform ion cyclotron resonance mass spectrometry [17]. In another study, factors that affected gas phase stabilities of non-covalent protein-peptide complexes were interrogated but without determining strengths of interactions [18].

Here, we describe a method to estimate apparent activation energies of dissociation of charged protein-protein complexes in the gas phase ($E_{A\,m0g}^{\#}$) directly under quasi-equilibrium conditions. After protein-protein complexes have been formed in solution, electrospray mass spectrometry is used to ionize and transfer them into the gas phase intact. Upon ion mobility separation of the ionized intact complexes from excess non-complexed constituents, dissociation of the complexes is initiated. Relative intensities of ion signals were used to calculate apparent activation energies of dissociation in the gas phase according to the Rice-Ramsperger-Kassel-Marcus quasi-equilibrium theory (RRKM/QET), which assumes that dissociation of molecular complexes in the gas phase is unidirectional and irreversible, i.e. not reaching equilibrium conditions. The energy that is applied to dissociate a protein-protein complex in the mass spectrometer is, thus, in correlation with its activation energy [19-21].

To develop our method, we investigated dissociation of the streptavidin tetramer and applied the procedure to three closely related protein-protein complexes consisting of Fc parts of immunoglobulins (IgG) and protein G´ isoforms (IgG-Fc•protein G´e, IgG-Fc•protein G´f, and IgG-Fc•protein G´g). Apparent activation energies of dissociation in the gas phase were compared with thermodynamic data from in-solution measurements.

## Materials and methods

### Materials

Protein G´e was obtained from Sigma-Aldrich, Steinheim, Germany (catalog no. P4689-5MG; lot no.SLBB8536V). Protein G´f was produced by the University of Applied Sciences Bonn-

Rhein-Sieg (Bonn, Germany). Protein G´g was a gift from Rainin Corp. (Oakland, California, USA). Active human IgG-Fc fragment was from Abcam, Cambridge, UK (product no. ab90285, lot no. GR149467-12). As supplied, all stock solutions contained 50 µg of protein. Polyclonal intravenous immunoglobulins (IVIG) were obtained from Omrix Biopharmaceuticals (Nes-Ziona, Israel). 16-Mercaptohexadecanoic acid, phosphate buffered saline powder, ethanolamine, N-hydroxysuccinimide, 2- [N-Morpholino] ethanesulfonic acid, 1-ethyl-3-[3-dimethylamino-propyl] carbodiimide were from Sigma-Aldrich. Details on streptavidin can be found in the Electronic Supplementary Material (ESM).

## IgG-Fc and protein G´-containing solutions

Solutions of active human IgG-Fc and protein G´ isoforms (protein G´e, protein G´f, and protein G´g) were buffer-exchanged using Amicon ultra centrifugal filters with 10 K cutoff (Millipore Corporation, Ireland) according to the manufacturer's protocol. Protein concentrations (aliquots of ca. 2 µg in 50 µl, each) were determined with the fluorescence-based Qubit™ assay (Invitrogen, Carlsbad, USA). For calibration, Qubit™ working solution (Qubit™ reagent diluted 1/100 in Qubit™ buffer) and three calibration standards (0, 200 and 400 ng/µl) were mixed (190 and 10 µl, respectively), incubated for 15 min and measured in the Qubit® 2.0 Fluorimeter. Raw fluorescence values were used to calculate the concentrations of the similarly treated proteins in the assay tubes and in the original stocks. Typical protein concentrations were between 0.2 µg/µl and 0.6 µg/µl. Sample solutions were either directly used for preparation of complexes consisting of protein G´ isoforms and IgG-Fc, or stored at -20 °C.

## Protein G´ - IgG-Fc complex preparations

IgG-Fc (3.6 µM; ca. 20-35 µl) in 200 mM ammonium acetate buffer, pH 7.1, was mixed with one buffer-exchanged protein G´ isoform at a time (ca. 6.5-13 µl) to yield a molar ratio of 1:1.3 (protein G´ isoform : IgG-Fc). Small excess of protein G´ was found to be optimal for both, generating an in-solution complex with 1:1 stoichiometry and avoiding precipitation. All

protein G´ isoform – IgG-Fc complexes were prepared in this manner at room temperature. Solutions with protein-protein complexes were either directly used for nano-ESI-IMS-MS/MS analysis, or kept at +4°C for maximally one week.

## Nano-ESI-IMS-MS/MS acquisition conditions

Capillaries for nano-ESI-IMS-MS/MS measurements were prepared in-house [22] from borosilicate glass tubes of 1 mm outer and 0.5 mm inner diameters using a P-1000 Flaming / Brown™ Micropipette Puller System (all Sutter Instrument, Novato, CA, USA) and gold-coated using a BalTec SCD 004 sputter coater (Bal-Tech, Balzers, Liechtenstein). For each measurement, 3 µl of sample were loaded using a micro-loader pipette tip (Eppendorf, Hamburg, Germany). Measurements were performed on a Synapt G2-S mass spectrometer (Waters MS-Technologies, Manchester, UK) equipped with a traveling-wave ion mobility cell (TW-IMS). The instrumental parameters were optimized as follows: source temperature, 50 ˚C; sample cone, 150 V; source offset, 150 V; trap collision energy, 4 V; trap DC bias, 45 V; trap gas flow, 10 ml/min; helium cell gas flow, 180 ml/min; IMS gas flow, 80 ml/min; wave velocity, 700 m/s; wave amplitude, 35 V. The capillary voltage was adjusted individually for each measurement (1.3 – 2 kV). The transfer collision energy (TCE) was raised from 2 V to 220 V in a stepwise manner (20-30 V steps) to induce protein-protein complex dissociation. Mass spectra were acquired in positive-ion mode applying a mass window of m/z 200-10,000. External mass calibration was performed with 1 mg/ml sodium iodide dissolved in an isopropanol / water solution (50:50, v/v). Data acquisition and processing was performed with the MassLynx software version 4.1 (Waters MS-Technologies, Manchester, UK) [22]. Data analysis and calculation of gas-phase activation energy is outlined in the ESM.

## In-solution $K_D$ value determinations

Real time bio-affinity analyses were performed with the K5 S-Sens® SAW biosensor (SAW Instruments, Bonn, Germany). The chip surface was cleaned by a 45 min sonication in 20 ml

piranha solution (30 % $H_2O_2$ : $H_2SO_4$; 1:1), and subsequent 15 min washing steps with ca 20 ml deionised water and with ca 20 ml ethanol, respectively. When dried, the plain gold surface of the chip was functionalised by incubating the chip in 30 ml 10 µM 16-mercaptohexadecanoic acid in $CHCl_3$ at 25 °C for 12 - 16 h to generate the self-assembled monolayer (SAM). Afterwards the SAM was washed with ca 5 ml ethanol and the chip was allowed to dry. The functionalized chip was inserted into the sensor unit of the instrument and immobilization of the antibody (ligand) was performed online in the microfluidic cell of the biosensor as follows. After washing with immobilisation buffer (10 mM acetate buffer, pH 5) for 30 min, 250 µl of 30 mg/ml EDC (dissolved in a mixture of 100 mM NHS : 50 mM MES, pH 6.3) were injected to activate the free carboxyl groups on the SAM. Ligand molecules were immobilized by injecting 250 µl of IVIG (2.5 µg/µl in 10 mM acetate buffer, pH 5). Remaining active sites were quenched by injecting 250 µl of aqueous 1M ethanolamine (pH 8.5). A flow rate of 20 µl/min was maintained throughout the immobilisation procedure. Binding experiments were performed at 22 °C using 10 mM PBS (pH 7.4) running buffer in a two frequency mode (optimum frequency: 150.8 MHz). Serial dilutions of analytes were prepared after determining stock solution concentrations (1200 nM, each) using the Qubit® 2.0 Fluorometer (Invitrogen, Carlsbad, USA) as described above. Sample concentrations of 25, 50, 100, 400, and 500 nM (protein G´e), 50, 200, 300, 400, and 500 nM (protein G´f) and 100, 300, 400, 600, and 800 nM (protein G´g), all in 10 mM PBS (pH 7.4) were used. The measurements (binding curves) were recorded as changes in the phases of the acoustic waves (in degree) due to binding as functions of time (in seconds). Data analysis procedures are described in the ESM.

## Results

### Method Development

To develop a mass spectrometry-based method by which apparent dissociation energies of ionized protein-protein complexes could be investigated in the gas phase, we analyzed the dissociation behavior of streptavidin tetramer complexes. Both, theoretical considerations as

well as details of our development-oriented investigations are provided in the ESM (Figs. S1 to S6). The main findings of our studies with streptavidin are that the RRKM/QE theory can be applied to describe the dissociation behavior of protein-protein complexes in the gas phase semi-quantitatively and that there is no need to investigate the dissociation behavior of each individual charge state of the protein-protein complex ions separately in order to deduce the apparent activation energy of complex dissociation. Instead, it is easier to perform and well suitable for calculating dissociation energies when all multiply charged ions of a protein-protein complex are simultaneously submitted to dissociation. The abundance-weighted mean of charge states of a protein-protein complex (i) can easily be determined as the maximum position of its precursor ion peak ensemble and (ii) is subsequently applied for all thermodynamic calculations.

## Analysis of individual proteins and formation of protein G´ complexes with IgG-Fc in-solution

Having established the procedure, we focused on the analysis of gas phase dissociation of protein-protein complexes consisting of the Fc parts of immunoglobulins (IgG-Fc) and one of three closely related protein G´ variants (proteins G´e, G´f, and G´g). Each protein G´ molecule contains three independent IgG-binding domains, which according to X-ray crystallography data [23] form part of the binding interface. Amino acid sequence alignment of the three protein G´ variants (ESM Fig. S7) shows that protein G´e and protein G´g have identical sequences of the so-called IgG-binding domains I, II, and III as well as of the in-between spacer sequences. They differ only in their flanking sequences that are located on either the N-terminus (protein G´e; FSN) or on the C-terminus (protein G´g; FSC). By contrast, proteins G´f and G´e possess similar N-terminal flanking sequences (FSN), but differ markedly by single amino acid exchanges in the IgG-binding domains (four of them in the relevant region). The introduced single amino acid exchanges of protein G´f have been suggested to increase the overall stability of protein G´f under basic conditions as compared to that of protein G´e [24]. All in all, the parts of proteins G´e and G´g relevant for IgG-binding

are identical as opposed to protein G'f. Comparable IgG binding properties are therefore expected for proteins G'e and G'g, but a different one for protein G'f.

When the free proteins G' were sprayed from neutral solutions, multiply charged ion series of high intensities with the highest signals at +10 (G'e) and +9 (G'f and G'g) were observed. Occasionally highly charged, i.e. unfolded proteins were detected as well with, however, only low signal intensities (ESM Fig. S8A-C). Protein G´e and protein G´f are known to be partially gluconoylated [25], yielding satellite ion signals of these protein species which are not always well-resolved when sprayed under native ESI conditions (ESM Fig. S8A-B). For the non-gluconoylated proteins we determined molecular masses, which closely agree with the calculated average masses of these proteins that were obtained from their amino acid sequences (Table 1).

When IgG-Fc was analyzed by nano-ESI-MS under neutral pH conditions, only a few rather broad protein ion signals were observed in the higher m/z range corresponding to charge states between 12+ and 15+ with a maximum intensity between the 13+ and the 14+ signal (ESM Fig. S8D). From these ions the average molecular mass of ca. 53,4 kDa was experimentally determined. We had used IgG-Fc from a pool of polyclonal human IgGs, so several IgG-Fc species were present with amino acid sequence differences and heterogeneous glycosylation, explaining the broad ion signals in the ESI-MS spectra.

Protein G´ isoforms were mixed with IgG-Fc at neutral pH (7.1), and the resulting protein-protein complexes were analyzed by nano-ESI-MS (Table 1). All three IgG-Fc•Protein G´ complexes adopted a 1:1 stoichiometry, and their charge state distributions followed the same trends as did the free protein G´ variants (Figure 1). Because of slight excess of protein G´ in the mixtures, multiply charged ion signals of free protein G´ variants were seen in the mass spectra as well.

## Dissociation of protein G´ - IgG-Fc complexes in the gas phase

The presence of potentially interfering free protein G´ ion signals led us to introduce a filtering step prior to inducing dissociation of the IgG-Fc•protein G´ complexes. We filtered

out ion signals of the unbound protein G´ isoforms by ion mobility separation. The specific arrival time windows in which the IgG-Fc•protein G´ complex ion signals were found exclusively, were determined when collision energy in the transfer cell was turned off. For dissociation analyses without interference of either ion signals of unbound protein G´ or of free IgG-Fc the respective arrival time windows were kept constant and acceleration voltages in the transfer cell ($V_{acc}$) were raised stepwise from 50 V to 220 V. For the IgG-Fc•protein G´e complex, exclusively ion signals of the complex with charge states from 16+ to 19+ were found until a transfer collision energy voltages ($V_{acc}$) of 70 V (Figure 2 A). The abundance-weighted mean charge state (m) of this complex was 17.40+ (Table 1).

Upon further increases of $V_{acc}$, the signal intensities of the complex ions decreased, while those of dissociated constituents appeared and increased (Figure 2 B-D). Protein G´e, which is the complex constituent with lower molecular mass, retained relatively more charges than the larger IgG-Fc. Released protein G´e carried 13+ to 11+ charges, whereas IgG-Fc retained 6+ or 7+ charges with low intensities. It should be mentioned that at very high transfer cell energies ($V_{acc}$ 220 V; cf. Figure 2 E) substantial peptide backbone cleavage occurred, producing poorly resolved fragment ions. All gas phase dissociation experiments were performed in triplicate for each of the three complexes. Abundance-weighted mean charge states (m) of 17.71+ and 16.33+ were calculated from the charge state distributions of IgG-Fc•protein G´f and IgG-Fc•protein G´g complexes, respectively (Table 1).

Using the series of mass spectra that were recorded with different transfer cell energies, i.e. different center-of-mass energies of the protein-protein complexes, we next determined all areas under the ion signals in a given spectrum that were present with decent intensity. After summing up all these areas under the ion signals, e.g. of protein G´e, the IgG-Fc•protein G´e complex, and their fragments, the ion signal intensities were normalized to the sum of all peak areas. The same procedure was applied with the IgG-Fc•protein G´f and IgG-Fc•protein G´g complex dissociation analyses (ESM Figs. S9 and S10). Normalized and averaged areas under the signals (norm. AUS) corresponding to the IgG-Fc•protein G´e complex and its dissociation products were plotted against center-of-mass collision energy values ($E_{com}$)

(Figure 3). The data points were fitted to a sigmoidal curve and showed the disappearance of the IgG-Fc•protein G´e complex with increasing energy while the intensities of the ion signals for the dissociated protein G´e went up to reach a maximum at around $E_{com}$ = 1.5 eV. At higher $E_{com}$ the ion signal intensities of the backbone fragments increased at the expense of the intact proteins. Dissociation analysis was performed for IgG-Fc•protein G´g and IgG-Fc•protein G´f complexes following the same procedure as described above.

The overlaid normalized AUS curves of all three IgG-Fc•protein G´ complexes (Figure 4 A) showed similar sigmoidal characteristics of complex disappearance with increasing $E_{com}$ values. The center-of-mass energy at which 50 % of the IgG-Fc•protein G´e and IgG-Fc•protein G´g complexes were dissociated was 1.3 eV. Yet, in case of the IgG-Fc•protein G´f complex 50 % dissociation was achieved already at 1.2 eV (Table 2).

Using the normalized AUS values we calculated the apparent Gibbs free energy, $\Delta G_g^{\#}$, in the gas phase for individual complex dissociation events and plotted them *vs.* $E_{com}$ (Figure 4 B). Interestingly, the slopes ("n-values") of all three fitted lines were very similar. A Linear Free Energy (LFE) evaluation, i.e. linear extrapolation of the lines from the $\Delta G_g^{\#}$ values provided the apparent activation energy ($E_{A\,m0g}^{\#}$) of protein-protein complex dissociation at the intercepts with the y-axis ($E_{com}$ = 0 eV), at which the external energy component is negligible.

It is apparent that the IgG-Fc•protein G´f complex requires less activation energy for dissociation than the IgG-Fc•protein G´e and IgG-Fc•protein G´g complexes, respectively. They both dissociate at comparable activation energies (Table 2). Since the IgG-Fc•protein G´f complex was found to be less stable in the gas phase than the complexes with the two other protein G´ isoforms, we conclude that amino acid sequence differences in the IgG-binding domains played more dominant roles for complex stability as opposed to the flanking sequences which seemed to be of lesser importance.

## Structural analysis of IgG-Fc complex formation by protein G´

From X-ray data of protein G´ it is known that IgG-binding domain III is involved in binding to IgG-Fc to a larger degree than the other two domains. Since mixing of protein G´ and IgG-Fc in solution resulted in a 1:1 stoichiometry, we conclude that the 3rd domain of protein G´ variants made the most important contacts to IgG-Fc. Consequently, the differences in amino acid sequences of the 3rd domains (Figure 5) between protein G´e or protein G´g and protein G´f were mostly to be made responsible for the observed protein-protein complex stability differences.

As outlined above, the amino acid sequences of the IgG-binding-relevant regions of protein G´e and protein G´g are identical (Figure 5, the two upper- and lowermost lines, respectively). Significant deviations within the actually binding-relevant regions only occur in the third IgG-binding domain of protein G'f as compared to the other two protein G´variants (Figure 5, the two innermost lines). Out of the four amino acid residues which differ in the IgG-binding regions of protein G´e or protein G´g as compared to protein G´f, residue E24 (boxes marked 1 and 1´ in Figure 5) has been suggested to make the largest difference. E24 is involved in hydrogen bonds with residues R255 and/or K248 of IgG-Fc. Disrupting these hydrogen bonds, the E24A exchange results in decreased binding strength of protein G´f to IgG-Fc. By contrast, amino acid exchanges A29V and N37A (boxes marked 2 and 2´ as well as 3 and 3´ in Figure 5) do not affect binding, because the concerned amino acid residues are too remote from the interface region between the two proteins. Finally, the carboxyl group of E42 (boxes marked 4 and 4´ in Figure 5) is involved in hydrogen bonding with the side chain of Q311 on the Fc part. Yet, it was reasoned that the E42V exchange neither favored nor disfavored binding, as upon this exchange remote conformational changes occurred and led to new hydrophobic interactions between protein G´ and IgG-Fc [23].

## In-solution dissociation constants of protein G´ - IgG complexes and comparison to gas phase activation energies

To test whether the differences in gas phase binding between protein G´ isoforms and IgG-Fc are mirroring in-solution behavior, we determined the dissociation constants ($K_{D\ s}$) of the interactions between polyclonal intravenous immunoglobulins (IVIG) and the three protein G´ isoforms using a Surface Acoustic Wave Biosensor assay. The average $K_{D\ s}$ for IgG - protein G´e binding obtained from four independent measurements in two measurement series was 54.8 ± 8.3 nM. For IgG interaction of protein G´f an average $K_{D\ s}$ value of 133.0 ± 17.5 nM and for protein G´g an average $K_{D\ s}$ value of 56.0 ± 2.8 nM was obtained from two independent measurements, each (Table 2). While the $K_{D\ s}$ values for protein G´e and protein G´g were identical within experimental error, that of protein G´f was roughly twice as high.

The experimentally determined apparent gas phase activation energy values ($E^{\#}_{A\ m0g}$) were mathematically transformed into apparent gas phase dissociation constants ($K^{\#}_{D\ m0g}$). Interestingly the trends of the gas phase values pretty much resembled those from the in-solution analyses. The $K^{\#}_{D\ m0g}$ values of IgG-Fc•protein G´e and IgG-Fc•G´g were more or less equal and half of that of IgG-Fc•protein G´f (Table 2), again indicating the differences in the binding strengths of the IgG-Fc•protein G´f complex as compared to the other two complexes.

## Discussion

The current study opens the field for rapidly and reliably investigating protein-protein complex stabilities in the gas phase using mass spectrometry. Non-covalent complex dissociation under CID conditions requires an energy input above a critical threshold and proceeds irreversibly, but (comparatively) slowly. This concerns the fraction of particles, which, according to the energy – dependent Boltzmann distribution, contain sufficient energy for crossing the dissociation energy barrier. Hence, within this “transition energy region” dissociated complex constituent ions (products) and protein-protein complex ions (educts) are detectable simultaneously with their respective relative abundances. So, despite the *de*

*facto* irreversible character of the dissociation reaction, an apparent equilibrium exists (RRKM-QET).

Of note, $E_{com50}$ values do not represent pure internal energies of protein-protein complexes, as they still contain the ions´ kinetic energy and charge-related energy increments. This may explain why in previous reports [26,27] experimentally determined gas phase binding strengths did not match with in-solution binding forces. Hence, for semi-quantitative evaluation of gas-phase protein-protein complex dissociation we emphasize to subtract the ions´ charge-related and kinetic energy contributions to the dissociation reaction, i.e. correct for "external" energy increments, by extrapolation to $E_{com} = 0$. The linear fit errors by which the intercepts with the y-axis are determined are within the 10% accuracy of the extrapolation procedure [28,29]. Increasing the number of repetitions renders the method more robust. To limit the inherent effort, abundance-weighted mean charge states (m) were successfully applied instead of individual charge state analyses.

As shown here, dissociation energies of protein-protein complexes in the gas phase that have been corrected for "external energy" contributions seem to represent in-solution properties of protein-protein complexes well. As was pointed out in a recent review [30], surface induced dissociation (SID) seems to be an alternative to CID breakage of non-covalent bonds in the gas phase [31,32]. However, in SID experiments charges are distributed proportionally to the masses of dissociated constituents [33]. Dissociation reactions of any kind traverse at least one transition state with its associated energy barrier. This principle applies to both, solution [34,35,28] and gas-phase reactions [36,37], thus providing a common thermodynamic background to both of them. In solution the backward reaction ensures that under equilibrium the system is limited by the Gibb's free energy, i.e. the internal energy difference between product and educt. However, in the gas phase, since there is no backward reaction, this role is fulfilled by the Gibb's free activation energy (here: $E^{\#}_{A\,m0g}$), representing the energy barrier between ground state and transition state. Both, gas phase and in-solution reactions assume, with first approximation, linear responses of product formation with changing complex energies, thus, nominal stability values can be obtained by

linear extrapolation [38,39]. This model assumes that dissociation is mostly enthalpy driven and not requiring substantial entropy energy terms (hard spheres model), and that transition states are comparable, if not independent, of the ions´ charge states. Yet, applying well-established in-solution equilibrium description (i.e. LFE; see ESM) to inherently irreversible gas-phase dissociation processes needs to take into account typical gas phase reaction features, such as asymmetric charge partitioning [40-43] and simultaneous (partial) unfolding of the dissociated complex components [44,26].

Applying the LFE concept to describe gas phase dissociation of protein-protein complexes, i.e. nominal complex stability values ($E^{\#}_{A\,m0g}$), we were able to add experimental evidence to the assumption that particular amino acid residues of the IgG-binding domains of protein G´ variants play decisive roles in high affinity binding to IgG-Fc. Our gas phase results not only confirmed, what was expected from previous knowledge, but also matched the results from in-solution measurements. Only, since desolvation occurs in the source of the mass spectrometer, hydrophobic interactions that contribute significantly to non-covalent binding in the liquid phase are (partially) lost in the gas phase. The (partial) loss of these hydrophobic forces could be the reason for lower binding constants observed in the gas phase ($K^{\#}_{D\,m0g}$) as opposed to the $K_{D\,s}$ values (cf. Table 2). However, since this is the first report on the issue, we do not exclude exceptions to the observations that have come out from our experiments. With respect to in-solution data, one should keep in mind that available software programs typically assume a 1:1 binding stoichiometry [45,46]. By contrast, our analyses of protein complexes by mass spectrometry provide definite protein-protein complex stoichiometries.

The method for experimental determination of gas phase stabilities of protein-protein complexes, as presented here, could, e.g., be used for checking whether or not non-synonymous coding Single Nucleotide Polymorphisms (nsSNPs) affect protein-protein interactions by comparing $E^{\#}_{A\,m0g}$ values of wild-type and mutated proteins. Altering protein function, particularly protein-protein interaction properties, ultimately may lead to disease [47,48]. The effects of nsSNPs, i.e. genomic mutations that cause specific amino acid substitutions [49], on binding strengths between two proteins can now be analyzed by ESI-

MS in detail. To emphasize the importance, it has been found that a nsSNP variant of integrin β-2 (CD18) caused a P178L exchange which affects binding to integrin α-X (CD11) [50]. Patients who carry this mutation in their genomes suffer from leukocyte adherence deficiency (LAD) [51,52]. LAD is clinically characterized by chronic neutrophilia, impaired wound healing, and severe life-threatening infections [53]. The huge amount of up to 200,000 nsSNPs in the human population shows the dimension of the task that awaits to be tackled, and, therefore, any method that helps to characterize stabilities of protein-protein interactions that is less time-consuming and less expensive as conventional methodology clearly is of importance to characterize these effects on protein functions [14].

In sum, determination of gas phase stabilities, i.e. apparent activation energies of dissociation ($E^{\#}_{A\ m0g}$) of protein-protein complexes in the gas phase is a rapid method to obtain useful information for characterizing protein-protein, protein-metabolite, protein-drug, or protein-nucleic acid interactions with only little sample consumption.

## Acknowledgements

We express our thanks to Dr. Stephan Mikkat for providing expertise on mass spectrometry. We also thank Dr. Marcus Frank for providing access to the capillary sputter. We acknowledge the German Academic Exchange Service (DAAD) for providing scholarships for YY (No. 91523785), BD (No. 91566064), and KO (No. 91548123). The WATERS Synapt G2S mass spectrometer has been bought through an EU grant (EFRE-UHROM 9) made available to MOG.

## Declaration on Conflict of Interest

The authors have no conflict of interest to declare.

## References

1. Przybylski M, Glocker MO (1996) Electrospray mass spectrometry of biomacromolecular complexes with noncovalent interactions - New analytical perspectives for supramolecular chemistry and molecular recognition processes. Angew Chem Int Edit 35 (8):807-826. doi:10.1002/anie.199608061

2. Loo JA (1997) Studying noncovalent protein complexes by electrospray ionization mass spectrometry. Mass Spectrom Rev 16 (1):1-23. doi:10.1002/(SICI)1098-2787(1997)16
3. Pagel K, Natan E, Hall Z, Fersht AR, Robinson CV (2013) Intrinsically Disordered p53 and Its Complexes Populate Compact Conformations in the Gas Phase. Angew Chem Int Edit 52 (1):361-365. doi:10.1002/anie.201203047
4. Bornschein RE, Ruotolo BT (2015) Ion mobility-mass spectrometry of charge-reduced protein complexes reveals general trends in the collisional ejection of compact subunits. Analyst 14 (20):7020-7029. doi:10.1039/c5an01242b
5. Chen F, Gulbakan B, Weidmann S, Fagerer SR, Ibanez AJ, Zenobi R (2016) Applying mass spectrometry to study non-covalent biomolecule complexes. Mass Spectrom Rev 35 (1):48-70. doi:10.1002/mas.21462
6. Hoaglund CS, Valentine SJ, Sporleder CR, Reilly JP, Clemmer DE (1998) Three-dimensional ion mobility/TOFMS analysis of electrosprayed biomolecules. Anal Chem 70 (11):2236-2242. doi:10.1021/ac980059c
7. Konijnenberg A, Butterer A, Sobott F (2013) Native ion mobility-mass spectrometry and related methods in structural biology. Biochim Biophys Acta 1834 (6):1239-1256. doi:10.1016/j.bbapap.2012.11.013
8. Sobott F, Benesch JL, Vierling E, Robinson CV (2002) Subunit exchange of multimeric protein complexes. Real-time monitoring of subunit exchange between small heat shock proteins by using electrospray mass spectrometry. J Biol Chem 277 (41):38921-38929. doi:10.1074/jbc.M206060200
9. Zhong YY, Hyung SJ, Ruotolo BT (2012) Ion mobility-mass spectrometry for structural proteomics. Expert Rev Proteomics 9 (1):47-58. doi:10.1586/Epr.11.75
10. Cooper A (1999) Thermodynamic analysis of biomolecular interactions. Curr Opin Chem Biol 3 (5):557-563. doi.org/10.1016/S1367-5931(99)00008-3
11. Robertson AD, Murphy KP (1997) Protein structure and the energetics of protein stability. Chem Rev 97 (5):1251-1267. doi:10.1021/Cr960383c
12. Erba EB, Barylyuk K, Yang Y, Zenobi R (2011) Quantifying Protein-Protein Interactions Within Noncovalent Complexes Using Electrospray Ionization Mass Spectrometry. Anal Chem 83 (24):9251-9259. doi:10.1021/ac201576e
13. Jorgensen TJD, Roepstorff P, Heck AJR (1998) Direct determination of solution binding constants for noncovalent complexes between bacterial cell wall peptide analogues and vancomycin group antibiotics by electrospray ionization mass spectrometry. Anal Chem 70 (20):4427-4432. doi:10.1021/Ac980563h
14. Krishnaswamy SR, Williams ER, Kirsch JF (2006) Free energies of protein-protein association determined by electrospray ionization mass spectrometry correlate accurately with values obtained by solution methods. Prot Sci 15 (6):1465-1475. doi:10.1110/ps.062083406
15. West GM, Tang L, Fitzgerald MC (2008) Thermodynamic analysis of protein stability and ligand binding using a chemical modification- and mass-spectrometry based strategy. Anal Chem 80 (11):4175-4185. doi:10.1021/ac702610a
16. Cech NB, Enke CG (2001) Practical implications of some recent studies in electrospray ionization fundamentals. Mass Spectrom Rev 20 (6):362-387. doi:10.1002/mas.10008
17. Sinelnikov I, Kitova EN, Klassen JS (2007) Influence of Coulombic repulsion on the dissociation pathways and energetics of multiprotein complexes in the gas phase. J Am Soc Mass Spectrom 18 (4):617-631. doi:10.1016/j.jasms.2006.11.006
18. Catalina MI, de Mol NJ, Fischer MJE, Heck AJR (2004) Probing factors affecting the gas phase stabilities of noncovalent complexes formed by peptides bound to the Grb2 SH2 domain protein. Phys Chem Chem Phys 6 (10):2572-2579. doi:10.1039/b315435a
19. Baer T, Mayer PM (1997) Statistical Rice-Ramsperger-Kassel-Marcus quasiequilibrium theory calculations in mass spectrometry. J Am Soc Mass Spectrom 8 (2):103-115. doi:10.1016/S1044-0305(96)00212-7
20. Rosenstock HM, Wallenstein MB, Wahrhaftig AL, Eyring H (1952) Absolute Rate Theory for Isolated Systems and the Mass Spectra of Polyatomic Molecules. Proc Natl Acad Sci USA 38 (8):667-678. doi:10.1073/pnas.38.8.667

21. Vekey K (1996) Internal energy effects in mass spectrometry. J Mass Spectrom 31 (5):445-463. doi:10.1002/(Sici)1096-9888(199605)31:5<445::Aid-Jms354>3.0.Co;2-G
22. Yefremova Y, Al-Majdoub M, Opuni KFM, Koy C, Yan Y, Gross ML, Glocker MO (2016) A Dynamic Model of pH-Induced Protein G ' e Higher Order Structure Changes derived from Mass Spectrometric Analyses. Anal Chem 88 (1):890-897. doi:10.1021/acs.analchem.5b03536
23. Sauer-Eriksson AE, Kleywegt GJ, Uhlen M, Jones TA (1995) Crystal structure of the C2 fragment of streptococcal protein G in complex with the Fc domain of human IgG. Structure 3 (3):265-278. doi.org/10.1016/S0969-2126(01)00157-5
24. Gulich S, Linhult M, Stahl S, Hober S (2002) Engineering streptococcal protein G for increased alkaline stability. Protein Eng 15 (10):835-842. doi:10.1093/protein/15.10.835
25. Yefremova Y, Al-Majdoub M, Opuni KFM, Koy C, Cui WD, Yan YT, Gross ML, Glocker MO (2015) "De-novo" amino acid sequence elucidation of protein G'e by combined "Top-Down" and "Bottom-Up" mass spectrometry. J Am Soc Mass Spectrom 26 (3):482-492. doi:10.1007/s13361-014-1053-2
26. Nesatyy VJ (2001) Gas-phase binding of non-covalent protein complexes between bovine pancreatic trypsin inhibitor and its target enzymes studied by electrospray ionization tandem mass spectrometry. J Mass Spectrom 36:950-959. doi:10.1002/jms.199
27. Nesatyy VJ (2002) Mass Spectrometry Evaluation of the Solution and Gas-phase Binding Properties of Noncovalent Protein Complexes. Int J Mass Spectrom 221:147-161. doi.org/10.1016/S1387-3806(02)00956-9
28. Pace CN, Shaw KL (2000) Linear extrapolation method of analyzing solvent denaturation curves. Proteins Suppl 4:1-7. doi:10.1002/1097-0134(2000)41:4+3.3.
29. Bolen DW, Santoro MM (1988) Unfolding free energy changes determined by the linear extrapolation method. 2. Incorporation of delta G degrees N-U values in a thermodynamic cycle. Biochemistry 27 (21):8069-8074. doi:10.1021/bi00421a014
30. Yefremova Y, Danquah BD, Opuni KFM, El-Kased RF, Koy C, Glocker MO (2017) Mass Spectrometric Characterization of Protein Structures and Protein Complexes in Condensed and Gas Phase. Eur J Mass Spectrom 23:in press. doi.org/10.1177/1469066717722256
31. Harvey SR, Yan J, Brown JM, Hoyes E, Wysocki VH (2016) Extended gas-phase trapping followed by surface-induced dissociation of noncovalent protein complexes. Anal Chem 88:1218–1221. doi:10.1021/acs.analchem.5b03479
32. Quintyn RS, Zhou MW, Yan J, Wysocki VH (2015) Surface-induced dissociation mass spectra as a tool for distinguishing different structural forms of gas-phase multimeric protein complexes. Anal Chem 87:11879–11886. doi:10.1021/ar400223t
33. Zhou M, Dagan, S., Wysocki, V.H.: (2012) Protein subunits released by surface collisions of noncovalent complexes: native-like compact structures revealed by ion mobility mass spectrometry. . Angew Chem Int Ed Engl 51:4336–4339. doi:10.1002/anie.201108700
34. Myers JK, Pace CN, Scholtz JM (1995) Denaturant m values and heat capacity changes: relation to changes in accessible surface areas of protein unfolding. Protein Sci 4 (10):2138-2148. doi:10.1002/pro.5560041020
35. Pace CN (1986) Determination and analysis of urea and guanidine hydrochloride denaturation curves. Methods Enzymol 131:266-280. doi:10.1016/0076-6879(86)31045-0
36. Drahos L, Vekey K (2003) Entropy evaluation using the kinetic method: is it feasible? J Mass Spectrom 38 (10):1025-1042. doi:10.1002/jms.538
37. Wu L, Lemr K, Aggerholm T, Cooks RG (2003) Recognition and quantification of binary and ternary mixtures of isomeric peptides by the kinetic method: metal ion and ligand effects on the dissociation of metal-bound complexes. J Am Soc Mass Spectrom 14 (2):152-160. doi:10.1016/S1044-0305(02)00868-1
38. Parker MJ, Spencer J, Clarke AR (1995) An integrated kinetic analysis of intermediates and transition states in protein folding reactions. J Mol Biol 253 (5):771-786. doi:10.1006/jmbi.1995.0590
39. Staniforth RA, Burston SG, Smith CJ, Jackson GS, Badcoe IG, Atkinson T, Holbrook JJ, Clarke AR (1993) The energetics and cooperativity of protein folding: a simple experimental analysis based upon the solvation of internal residues. Biochemistry 32 (15):3842-3851. doi:10.1021/bi00066a003

40. Benesch JL, Ruotolo BT, Simmons DA, Robinson CV (2007) Protein complexes in the gas phase: technology for structural genomics and proteomics. Chem Rev 107 (8):3544-3567. doi:10.1021/cr068289b
41. Jurchen JC, Williams ER (2003) Origin of asymmetric charge partitioning in the dissociation of gas-phase protein homodimers. J Am Chem Soc 125 (9):2817-2826. doi:10.1021/ja0211508
42. Sciuto SV, Liu JJ, Konermann L (2011) An Electrostatic Charge Partitioning Model for the Dissociation of Protein Complexes in the Gas Phase. J Am Soc Mass Spectrom 22 (10):1679-1689. doi:10.1007/s13361-011-0205-x
43. Sobott F, Robinson CV (2004) Characterising electrosprayed biomolecules using tandem-MS - the noncovalent GroEL chaperonin assembly. Int J Mass Spectrom 236 (1-3):25-32. doi:10.1016/j.ijms.2004.05.010
44. Benesch JL (2009) Collisional activation of protein complexes: picking up the pieces. J Am Soc Mass Spectrom 20 (3):341-348. doi:10.1016/j.jasms.2008.11.014
45. Dragusanu M, Petre BA, Slamnoiu S, Vlad C, Tu TT, Przybylski M (2010) On-Line Bioaffinity-Electrospray Mass Spectrometry for Simultaneous Detection, Identification, and Quantification of Protein-Ligand Interactions. J Am Soc Mass Spectrom 21 (10):1643-1648. doi:10.1016/j.jasms.2010.06.011
46. Gronewold TMA (2007) Surface acoustic wave sensors in the bioanalytical field: Recent trends and challenges. Anal Chim Acta 603 (2):119-128. doi:10.1016/j.aca.2007.09.056
47. Thomas PD, Kejariwal A (2004) Coding single-nucleotide polymorphisms associated with complex vs. Mendelian disease: Evolutionary evidence for differences in molecular effects. Proc Natl Acad Sci U S A 101 (43):15398-15403. doi:10.1073/pnas.0404380101
48. Zhao N, Han JG, Shyu CR, Korkin D (2014) Determining Effects of Non-synonymous SNPs on Protein-Protein Interactions using Supervised and Semi-supervised Learning. Plos Comput Biol 10 (5). doi:ARTN e1003592 10.1371/journal.pcbi.1003592
49. Stunnenberg HG, Hubner NC (2014) Genomics meets proteomics: identifying the culprits in disease. Hum Genet 133 (6):689-700. doi:10.1007/s00439-013-1376-2
50. David A, Razali R, Wass MN, Sternberg MJ (2012) Protein-protein interaction sites are hot spots for disease-associated nonsynonymous SNPs. Hum Mutat 33 (2):359-363. doi:10.1002/humu.21656
51. Back AL, Kwok WW, Hickstein DD (1992) Identification of two molecular defects in a child with leukocyte adherence deficiency. J Biol Chem 267 (8):5482-5487.
52. Ohashi Y, Yambe T, Tsuchiya S, Kikuchi H, Konno T (1993) Familial Genetic-Defect in a Case of Leukocyte Adhesion Deficiency. Hum Mutat 2 (6):458-467. doi:10.1002/humu.1380020606
53. Etzioni A (1996) Adhesion molecules - Their role in health and disease. Pediatr Res 39 (2):191-198. doi:10.1203/00006450-199602000-00001



## Figure legends

### Figure 1

NanoESI mass spectra of protein complexes derived from protein G´ isoforms and IgG-Fc. **A:**IgG-Fc•proteinG´e. **B:**IgG-Fc•proteinG´f. **C:**IgG-Fc•proteinG´g. Charge states and m/z values for selected ion signals are given for the complexes (right ion series) and for the respective uncomplexed protein G´ isoforms (left ion series). Solvent: 200 mM $NH_4OAc$.

## Figure 2

Nano-ESI mass spectra of IgG-Fc•proteinG´e after ion mobility separation and exposure to different transfer cell energies (TCE; given as acceleration voltages $V_{acc}$). **A:** 70 V. **B:** 120 V. **C:** 150 V. **D:** 170 V. **E:** 200 V. Charge states and m/z values for selected ion signals are given for the complexes (center ion series) and for the respective released protein G´e (left ion series) and IgG-Fc (right ion series). Solvent: 200 mM $NH_4OAc$. Ranges with 10-fold or 5-fold magnification are marked; m/z values of ion signal apexes are labeled. At 200 V TCE protein ion signals are superimposed by ion signals from fragments.

## Figure 3

Normalized areas under signals (AUS) plotted as a function of center-of-mass collision energy. AUS of IgG-Fc•proteinG´e (filled pentagons), intact protein G´e (filled triangles), and fragments (open pentagons) are shown. Each data point is the mean of three independent measurements and standard deviations are shown by vertical bars. A Boltzmann function was used to fit the curve for the IgG-Fc•proteinG´e complex, a Gaussian function was used to fit the curve for intact protein G´e, and a logistic function was used to fit the curve for the protein fragment abundances.

## Figure 4

**A:** Normalized areas under signals (AUS) plotted as functions of center-of-mass collision energy for IgG-Fc•proteinG´e (dashed line; filled squares), IgG-Fc•proteinG´g (dotted line; filled circles), and IgG-Fc•proteinG´f (solid line; empty squares). Curves are fitted using Boltzmann functions. **B:** Differences of apparent Gibbs free energies in the gas phase ($\Delta G_g^{\#}$) plotted as functions of center-of-mass collision energy for IgG-Fc•proteinG´e (dashed line; filled squares), IgG-Fc•proteinG´g (dotted line; filled circles), and IgG-Fc•proteinG´f (solid line; empty squares). The intercepts with the y-axis (zoomed insert) give $E_{A\,m0g}^{\#}$ values.

**Figure 5**

Partial amino acid sequences of protein G´e, protein G´g, and protein G´f regions that are involved in contacts with IgG-Fc. Amino acid exchanges in the 3rd domains are boxed and numbered.

**Table 1:** Average molecular masses of starting materials and protein-protein complexes.

| | protein | | | IgG-Fc•proteinG´ complex | |
|---|---|---|---|---|---|
| | **no. of aa** | **$M_r$** | **exp. mass ± stdv., Da** | **exp. mass ± stdv., Da** | **m** |
| G´e | 241 | 25999.55 | 25999.60 ± 0.09 | 79380.20 ± 53.94 | 17.40 |
| G´f | 228 | 24415.92 | 24415.05 ± 0.16 | 77818.48 ± 55.52 | 17.71 |
| G´g | 209 | 22809.09 | 22809.43 ± 0.10 | 76016.77 ± 20.73 | 16.33 |
| IgG-Fc | n.d. | n.d. | 53392.70 ± 0.83 | n.a. | n.d. |

aa: amino acid residues
m = abundance weighted mean charge state
n.d.; not determined
n.a.; not applicable

**Table 2:** Comparison of gas phase and in-solution parameters of protein G´ isoforms complexed with IgG(Fc).

| protein G´ | solution | gas phase | | |
|---|---|---|---|---|
| | $K_{Ds} \pm stdv.$ [nM] | $E_{com50}$ [eV] [a)] | $E_{A\,m0g}^{\#}$ $[\frac{J}{mol \bullet K}]$ | $K_{D\,m0g}^{\#}$ [nM] |
| G´e | 54.8 ± 8.3 | 1.3 | 135.7 | 81.6 |
| G´f | 133.0 ± 17.5 | 1.3 | 127.2 | 226.7 |
| G´g | 56.0 ± 2.8 | 1.2 | 133.1 | 111.5 |

a) center-of-mass energies at which 50 % of the IgG-Fc•protein G´ complexes were dissociated.

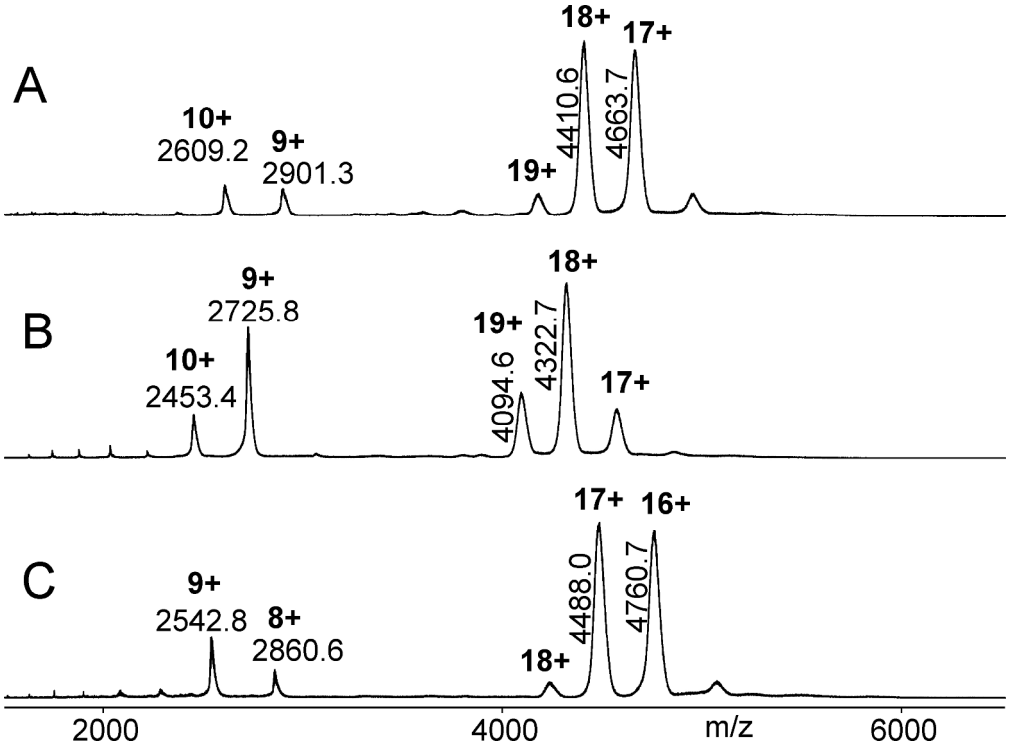


NanoESI mass spectra of protein complexes derived from protein G´ isoforms and IgG-Fc. A:IgG-Fc•proteinG´e. B:IgG-Fc•proteinG´f. C:IgG-Fc•proteinG´g. Charge states and m/z values for selected ion signals are given for the complexes (right ion series) and for the respective uncomplexed protein G´ isoforms (left ion series). Solvent: 200 mM NH4OAc.

257x189mm (300 x 300 DPI)

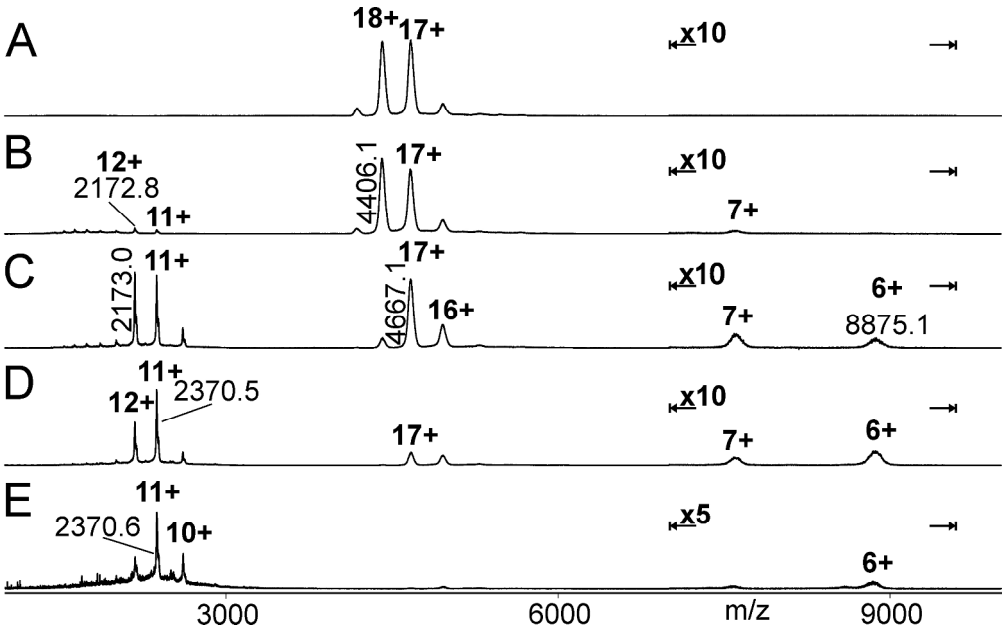


Nano-ESI mass spectra of IgG-Fc•proteinG´e after ion mobility separation and exposure to different transfer cell energies (TCE; given as acceleration voltages Vacc). A: 70 V. B: 120 V. C: 150 V. D: 170 V. E: 200 V. Charge states and m/z values for selected ion signals are given for the complexes (center ion series) and for the respective released protein G´e (left ion series) and IgG-Fc (right ion series). Solvent: 200 mM NH4OAc. Ranges with 10-fold or 5-fold magnification are marked; m/z values of ion signal apexes are labeled. At 200 V TCE protein ion signals are superimposed by ion signals from fragments.

274x169mm (300 x 300 DPI)

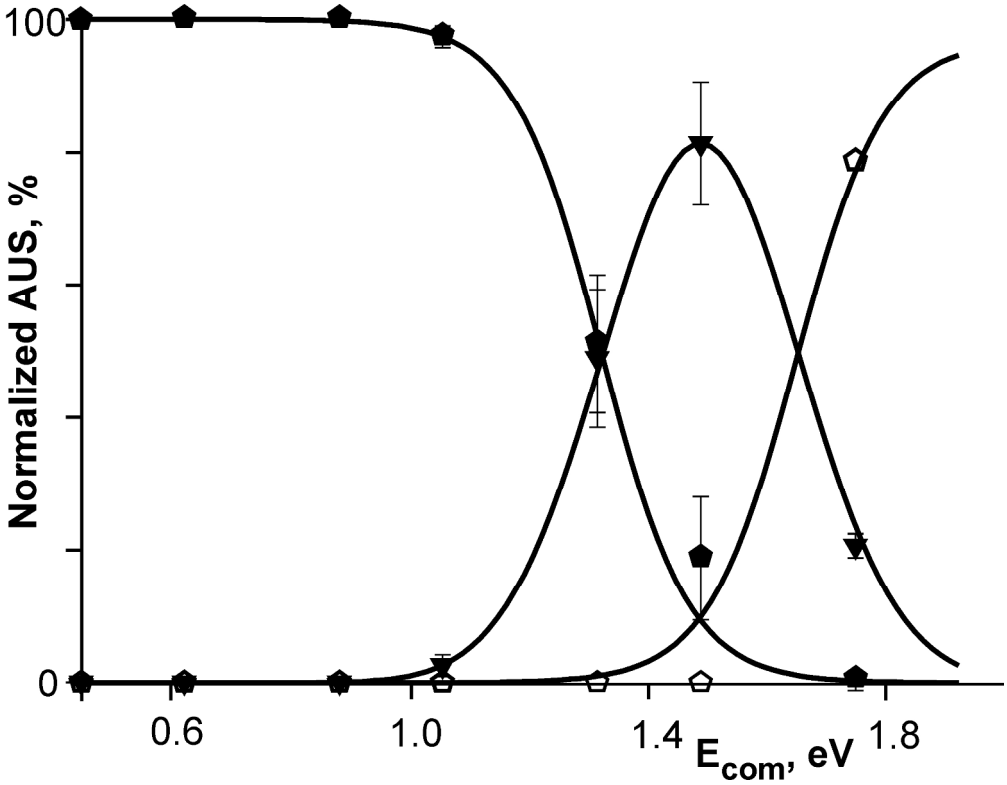


Normalized areas under signals (AUS) plotted as a function of center-of-mass collision energy.AUS of IgG-Fc•proteinG´e (filled pentagons), intact protein G´e (filled triangles), and fragments (open pentagons) are shown. Each data point is the mean of three independent measurements and standard deviations are shown by vertical bars. A Boltzmann function was used to fit the curve for the IgG-Fc•proteinG´e complex, a Gaussian function was used to fit the curve for intact protein G´e, and a logistic function was used to fit the curve for the protein fragment abundances.

244x189mm (300 x 300 DPI)

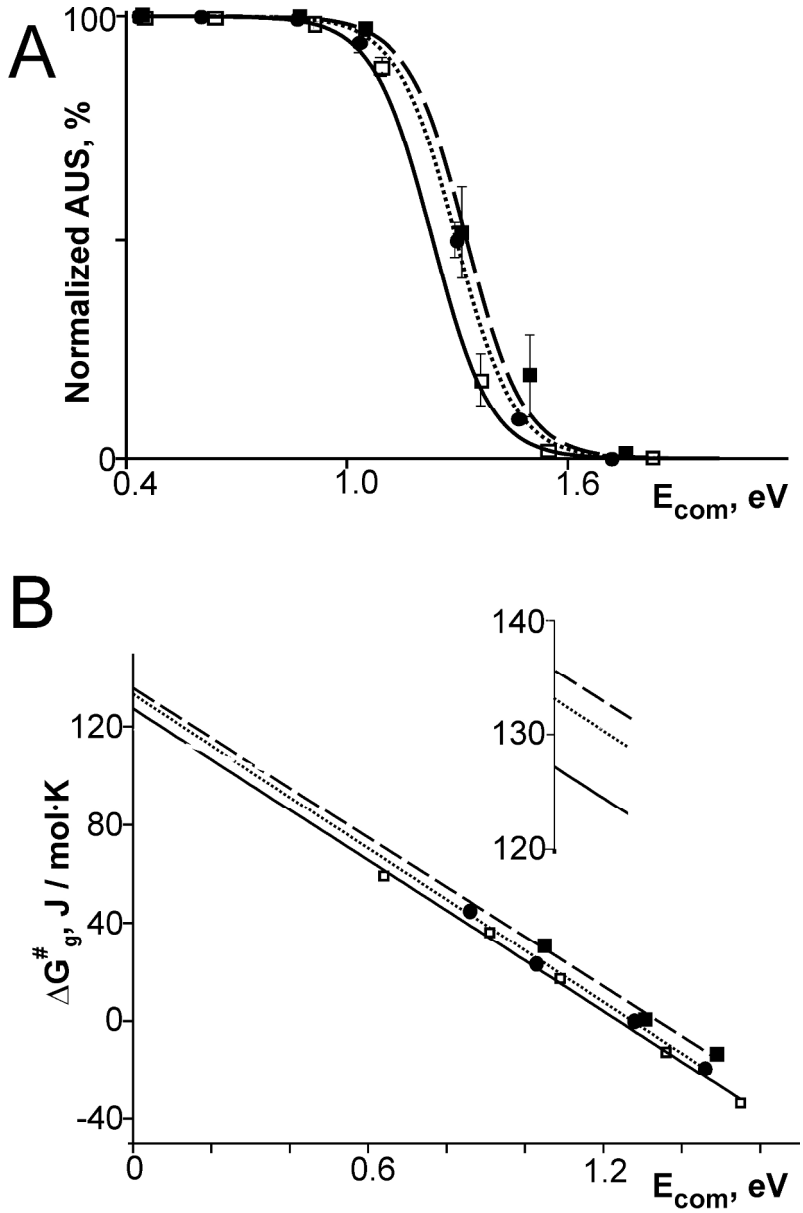


A: Normalized areas under signals (AUS) plotted as functions of center-of-mass collision energy for IgG-Fc•proteinG´e (dashed line; filled squares), IgG-Fc•proteinG´g (dotted line; filled circles), and IgG-Fc•proteinG´f (solid line; empty squares). Curves are fitted using Boltzmann functions. B: Differences of apparent Gibbs free energies in the gas phase (〖ΔG〗_g^( #)) plotted as functions of center-of-mass collision energy for IgG-Fc•proteinG´e (dashed line; filled squares), IgG-Fc•proteinG´g (dotted line; filled circles), and IgG-Fc•proteinG´f (solid line; empty squares). The intercepts with the y-axis (zoomed insert) give E_Ag^( #) values.

185x281mm (300 x 300 DPI)

Protein G´e / Protein G´g

```
                23          30                40
domain I        AATAEKVFKQYANDNGVDGEWT
domain II       AATAEKVFKQYANDNGVDGEWT
domain III      AETAEKAFKQYANDNGVDGVWT
                 1        2          3       4
```

Protein G´f

```
                1´       2´          3´      4´
domain III      AATAEKVFKQYANDAGVDGEWT
domain II       AATAEKVFKQYANDAGVDGEWT
domain I        AATAEKVFKQYANDAGVDGEWT
```

Partial amino acid sequences of protein G´e, protein G´g, and protein G´f regions that are involved in contacts with IgG-Fc. Amino acid exchanges in the 3rd domains are boxed and numbered.

246x140mm (300 x 300 DPI)

**Analytical and Bioanalytical Chemistry**

**Electronic Supplementary Material**

# Apparent activation energies of protein-protein complex dissociation in the gas phase determined by electrospray mass spectrometry

Yelena Yefremova, F. Teresa I. Melder, Bright D. Danquah, Kwabena F.M. Opuni, Cornelia Koy, Alexandra Ehrens, David Frommholz, Harald Illges, Knut Koelbel, Frank Sobott, Michael O. Glocker

## I) Theoretical background and method development



## II) Protein G´ • IgG-Fc

## I) Theoretical background and method development

### Basic considerations

Thermodynamic evaluation of gas-phase dissociation reactions of protein-protein complexes along well established laws for in-solution reactions, such as linear free energy relationships, is derived from considering the following facts and simplifications [17-21, 26, 27, 29, 30]:

1. Both, the protein-protein complex dissociation reaction itself (because of entropy gain of the products) and concomitant complex constituent unfolding reactions (due to lack of the hydrophobic effect which could drive refolding) are irreversible.
2. Within the energy "transition region" of the protein-protein complex dissociation reaction, the time required for recording single spectra is shorter than that which was needed for reaching complete unfolding/dissociation of protein-protein complexes.
3. Consequently, educt (protein-protein complex) and product (complex constituent) ion signals are simultaneously recorded in the corresponding mass spectra with elevated collision energies as opposed to the exclusive presence of educt ions in the "baseline region" as well as of only product ions in the maximum energy regime (disregarding potential fragmentation).

These considerations permit application of "Linear Free Energy relations" (LFE).

In-solution thermodynamic methods [10-16] were adapted to gas-phase experiments using the following conventions and definitions:

(1) $$\text{Normalized area under signal (norm. AUS)} = \left(f\,\frac{products}{educts}\right) * [\%] \quad (1)$$

(2) The charge contribution to the kinetic energy was accounted for by converting acceleration voltage ($V_{acc}$) into center of mass ($E_{com}$) energy:

$$E_{lab\ frame} = V_{acc} * z \quad (2)$$

$$E_{com} = \left(\frac{N}{m_p+N}\right) * E_{lab\ frame} \quad (3)$$

($N$ = mass of the neutral collision gas (here Ar, $M_r$ = 39.95); $m_p$ = mass of the protein-protein complex ion; z = charge)

(3) An "in-solution-like" LFE was applied to the "apparent equilibrium":

$$\Delta G_g^{\#} = -R * ln\left(\frac{100\%-norm.AUS}{norm.AUS}\right) = \Delta G_{m0g}^{\#} - \mathrm{n} * [E_{com}] \quad (4)$$

$R$ = gas constant, n = slope, m = mean of charge state, 0 = at $E_{com}$=0, g = gas phase. Principally, the absolute temperature, T, should be a factor in this equation, too, but since it cannot be determined with certainty, it was merged with the free enthalpy term. $\Delta G_{m0g}^{\#}$ must, therefore, be regarded as apparent.

(4) Extrapolation towards "zero activation", at $E_{com}$=0, yields the nominal stability (as opposed to observed parameters as threshold values) of complexes. However, because of the de facto irreversibility of the dissociation reaction (see above considerations), this value describes not a

thermodynamic (equilibrium) stability, but has to be regarded as being proportional to the activation energy ($E^{\#}_{A\,m0g}$): $\Delta G^{\#\,0}_{m0g} = E^{\#}_{A\,m0g}$ (5)

Plotting normalized AUS curves as functions of the respective lab frame or center-of-mass energies in order to obtain valid threshold energies has been accepted standard. But, Coulomb repulsion affects the unfolding and dissociation processes ("interface separation") of protein-protein complex ions in the gas phase. This dissociation process comprises two different aspects which need to be considered separately.

1) the charge impact on kinetic energy itself is conveniently corrected for by plotting the peak areas of complex ions and constituent ions, respectively, vs. lab frame or, as in our case, center-of-mass energies ($E_{com}$).
2) charge repulsion - as driving force for separation - is covered by our analysis by extrapolation towards $E_{com} = 0$.

Further correction is not necessary, since we used the respective educt and product abundances (in the transition region) at energies that limit formation of charge repulsed products. Principally, this simplification is correct as long as the procedure is applied to each charge state separately. Of note, our experiments with streptavidin have shown that extrapolation lines from the different charge states are well represented by the line that is obtained by the data from the mean of the charge states.

Therefore, we determined the activation energy ($E^{\#}_{A\,m0g}$) at $E_{com}$=0 eV of protein-protein complexes by applying "Linear Free Energy relations" (LFE; cf. Figure S6B).

**Ion mobility separation of protein complex ions**

Our method was tested by dissociating the streptavidin tetramer (S4) with and without ion mobility selection of individual charge states using a Synapt mass spectrometer as described in the Materials and Methods section. A streptavidin tetramer (S4) stock solution was prepared by dissolving the commercial product (Carl-Roth, Karlsruhe, Germany, article no. 6073, lot no. 025218507; Mr (avg.): 56,116) in 50 mM $NH_4OAc$, pH 6.9 (final streptavidin (S4) concentration 1 mg/ml). Buffer exchange, using 50 mM $NH_4OAc$, pH 6.9 for all steps, protein concentration determination, and spectrum acquisition are described in the materials and methods section for IgG-Fc and protein G´-containing solutions.

Despite the fact that the 16+ streptavidin tetramer ion signal is located at the same m/z position as the 4+ streptavidin monomer ion signal, there is no risk of ambiguity in the assignment, since the latter appears at clearly different TCE / $E_{com}$ values as opposed to that of the first one. When dissociating the individual charge states 15+ and 14+ of the tetramer complex there is no overlap of tetramer with monomer ions.

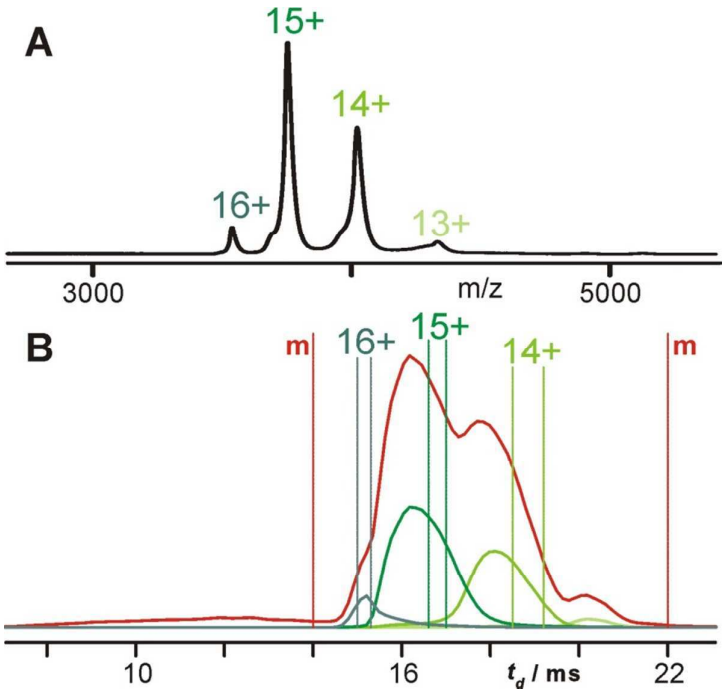


**Fig. S1** Ion mobility selection of tetrameric streptavidin ions. A: Precursor ion mass spectrum of the intact streptavidin tetramer recorded with 30 V acceleration voltage (TCE). Individual charge states are indicated above the respective peaks. B: Arrival time distributions corresponding to the complete spectrum (red) or to the individual charge states (same color code as in A). Drift time windows as used for abundance-weighted mean of charge states (m) and charge state-specific ion mobility selections (see Fig. S2-S5) are indicated by vertical ticked lines

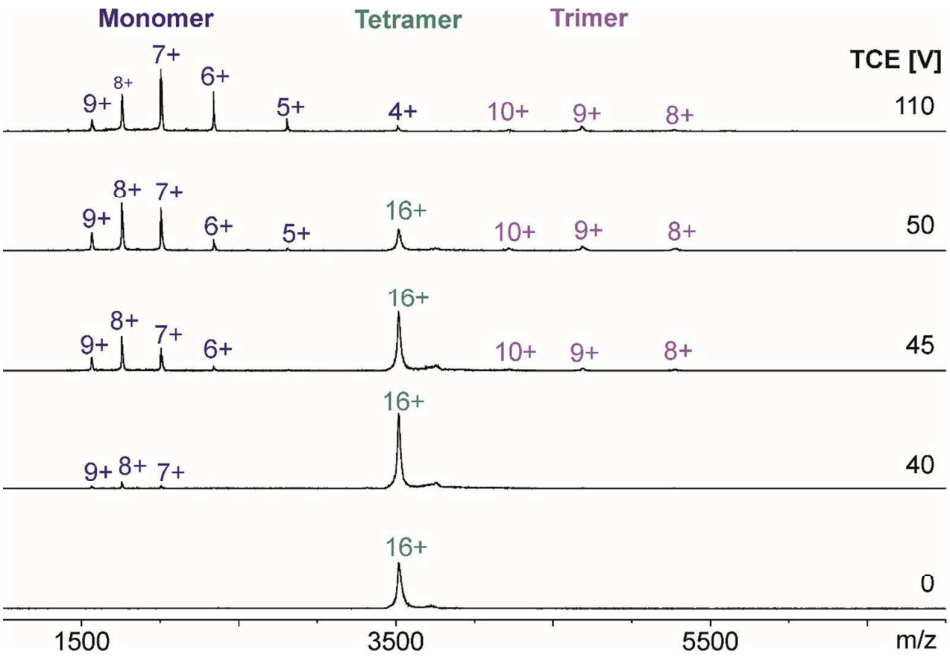


**Fig. S2** Collision induced dissociation of 16+ tetrameric streptavidin ion. NanoESI mass spectra of intact and dissociated streptavidin tetramers after ion mobility selection of the 16+ charge state and its subsequent collision induced dissociation by stepwise increasing transfer cell collision energies (TCE, from bottom to top)

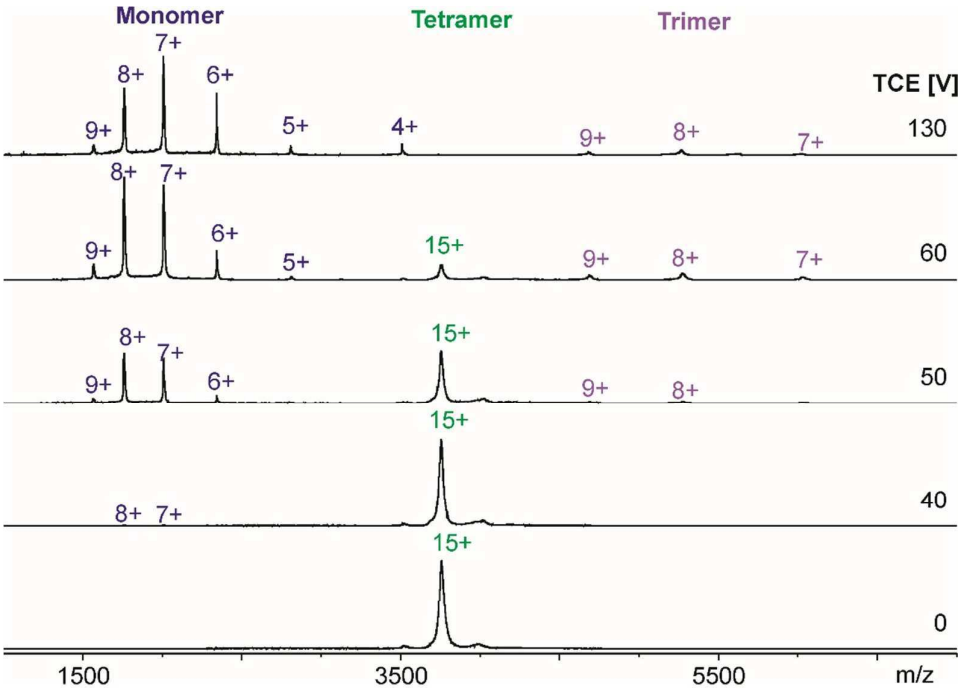


**Fig. S3** Collision induced dissociation of 15+ tetrameric streptavidin ion. NanoESI mass spectra of intact and dissociated streptavidin tetramers after ion mobility selection of the 15+ charge state and its subsequent collision induced dissociation by stepwise increasing transfer cell collision energies (TCE, from bottom to top)

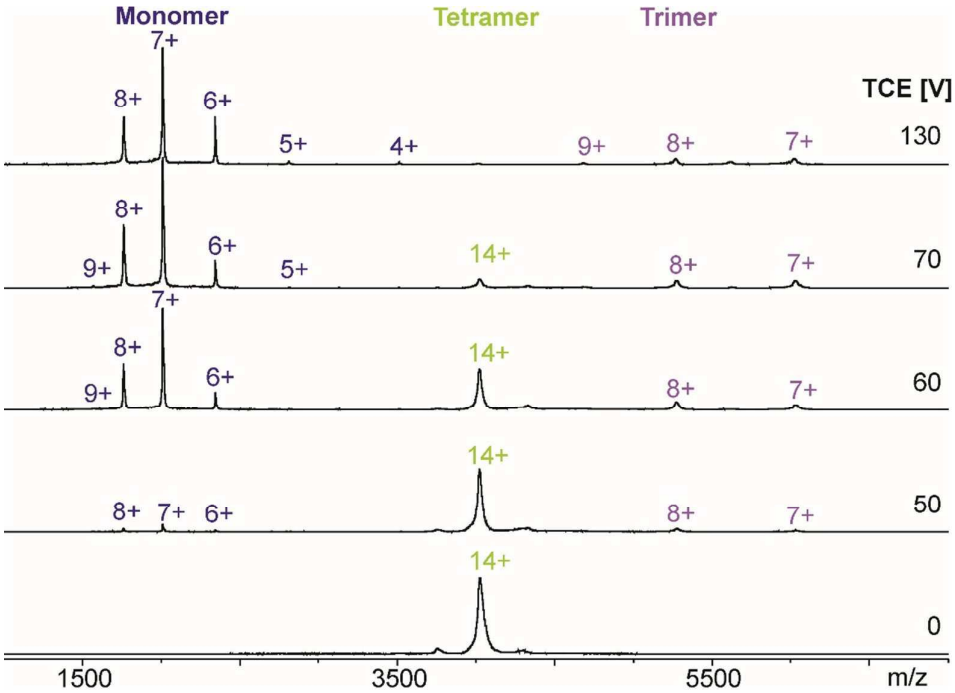


**Fig. S4** Collision induced dissociation of 14+ tetrameric streptavidin ion. NanoESI mass spectra of intact and dissociated streptavidin tetramers after ion mobility selection of the 14+ charge state and its subsequent collision induced dissociation by stepwise increasing transfer cell collision energies (TCE, from bottom to top)

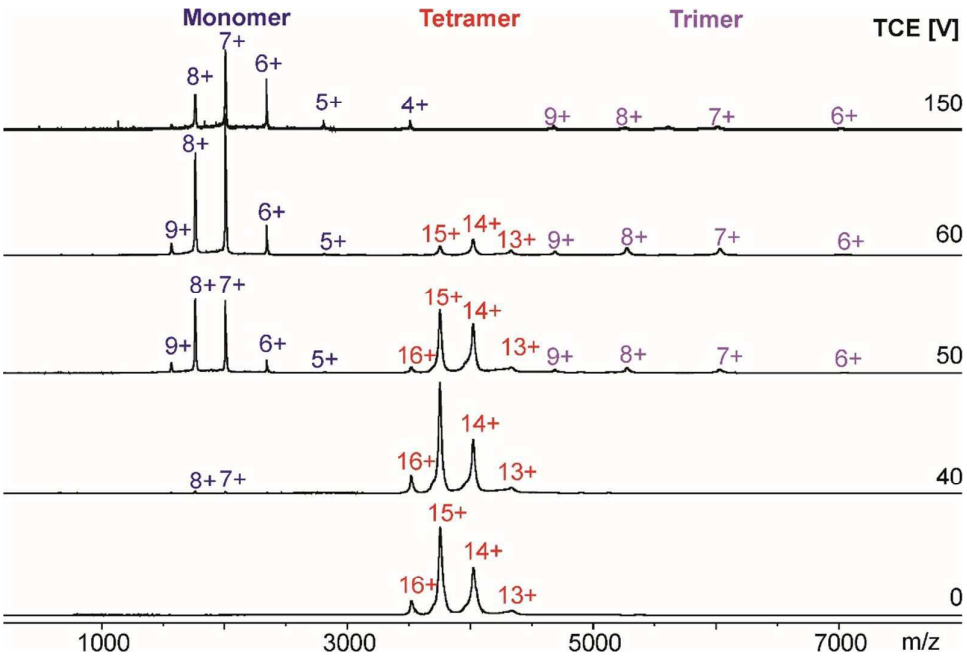


**Fig. S5** Collision induced dissociation of n+ tetrameric streptavidin ions. NanoESI mass spectra of intact and dissociated streptavidin tetramers after ion mobility selection of the abundance-weighted mean of charge states (m) and their subsequent collision induced dissociation by stepwise increasing transfer cell collision energies (TCE, from bottom to top)

**Evaluation of CID data of ion mobility-selected streptavidin complexes**

From Fig. S2-S5 the unaltered pattern of the highly charged monomeric product ions is apparent – regardless of precursor ion charge. Contrarily, the charge states of the respective precursor and dominant trimeric product ions correlate strictly. Since the classical asymmetric charge distribution pattern is adhered to, ion mobility selection can be conveniently used as surrogate of conventional MS/MS.

The unfolding/dissociation transitions of tetrameric streptavidin are steep (Fig. S6A), leaving only four to five data points for LFE evaluation. The potential error margin depends from either keeping or dropping the extreme points from analysis (Fig. S6B). Sufficient numbers of repetitions are therefore required. These, in turn, are more conveniently achieved for the complete sets of precursor ion peaks (m) than for each individual charge state. So, we widened the drift time window to encompass the complete tetrameric ensemble (+16 to +13, m; see Fig. S1) and measured dissociation of tetrameric streptavidin (S4) in triplicate (Fig. S5). An abundance-weighted mean of charge state (m) of 14.6+ was calculated using equation 6:

$$z = \sum z_n * \left(\frac{I_{z_n}}{\sum I}\right) \tag{6}$$

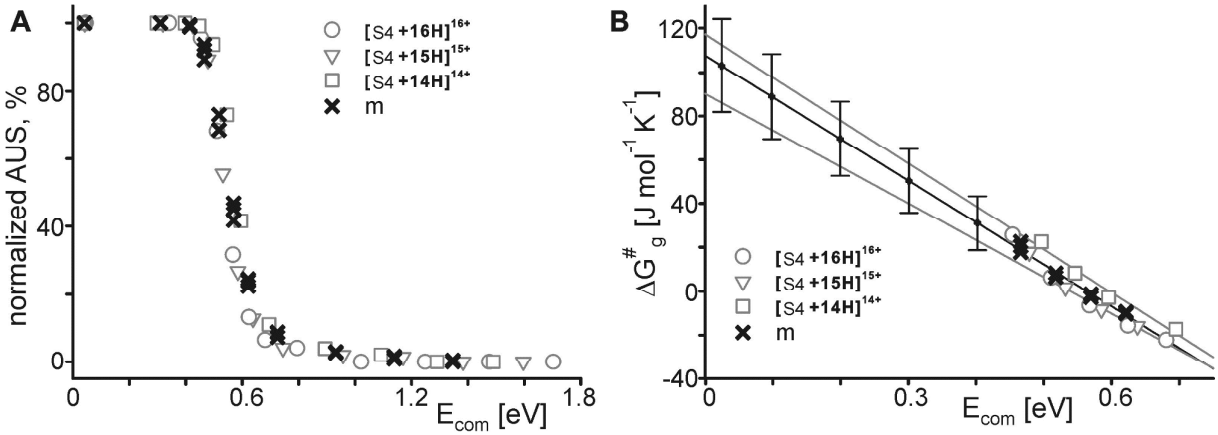


**Fig. S6** Evaluation of streptavidin complex gas-phase stabilities by LFE. A: Series of CID measurements using ion mobility-selected (see Fig. **S1** for the respective drift time windows) tetrameric streptavidin (S4) were conducted and normalized areas under ion signals (normalized AUS) were determined as described. B: LFE evaluation was applied to the normalized AUS data. Selected data points were deliberately dropped from analysis to test for their effects on resulting deviations (maximum effects are within error bars).

Quite reasonably – as the mean of charge states inherently represents the most intense signal within the considered ensemble (+14 and +15 for S4) – LFE evaluation of these data closely resembles the corresponding results of the individual charge state-specific measurements. And, since the most intense native-MS peaks of a given protein are usually adjacent to each other, LFE evaluation of abundance-weighted mean of charge states will yield fairly representative $E^{\#}_{A\,m0g}$ values for the complete charge state ensemble of a given protein-protein complex.

## II) Protein G´ • IgG-Fc

**Amino acid sequences of protein G´ variants**

```
                FSN                                                 domain I
Protein G'e     GSSHHHHHHSSGLVPRGSHMASMTGGQQMGRDPNSSSVDKLAAALETYKLILNGKTLKGE
Protein G'g     ---------------------------------------------GTYKLILNGKTLKGE
Protein G'f     GSSHHHHHHSSGLVPRGSHMASMTGGQQMGRG-------------STYKLILAGKTLKGE

                                                     spacer 1
Protein G'e     TTTEAVDAATAEKVFKQYANDNGVDGEWTYDDATKTFTVTEKPEVIDASELTPAVTTYKL
Protein G'g     TTTEAVDAATAEKVFKQYANDNGVDGEWTYDDATKTFTVTEKPEVIDASELTPAVTTYKL
Protein G'f     TTTEAVDAATAEKVFKQYANDAGVDGEWTYDDATKTFTVTEKPEVIDASELTPAVTTYKL

                domain II                                           spacer 2
Protein G'e     VINGKTLKGETTTEAVDAATAEKVFKQYANDNGVDGEWTYDDATKTFTVTEKPEVIDASE
Protein G'g     VINGKTLKGETTTEAVDAATAEKVFKQYANDNGVDGEWTYDDATKTFTVTEKPEVIDASE
Protein G'f     ILAGKTLKGETTTEAVDAATAEKVFKQYANDAGVDGEWTYDDATKTFTVTEKPEVIDASE

                     domain III
Protein G'e     LTPAVTTYKLVINGKTLKGETTTKAVDAETAEKAFKQYANDNGVDGVWTYDDATKTFTVT
Protein G'g     LTPAVTTYKLVINGKTLKGETTTKAVDAETAEKAFKQYANDNGVDGVWTYDDATKTFTVT
Protein G'f     LTPAVTTYKLILAGKTLKGETTTEAVDAATAEKVFKQYANDAGVDGEWTYDDATKTFTVT

                         FSC
Protein G'e     E-------------
Protein G'g     EKIAAALEHHHHHH
Protein G'f     E-------------
```

**Fig. S7** Amino acid alignment of the three protein G' variants. The amino acid sequences of proteins G'e, G'g and G'f (from top to bottom in each single panel) are aligned with the N- and C-termini shown in italics. Kinked arrows encompass the complete IgG binding domains, whereas boxes indicate regions known to be actually involved in IgG binding. Distinct domains and linkers of the proteins are labeled individually above the sequences: the N- and C-terminal flanking sequences (FSN and FSC, respectively), the three IgG binding domains (I-III) and the spacer regions in between. Residues, the exchanges of which distinguish protein G'f from the other two, are underlined

**Data on individual complex constituents**

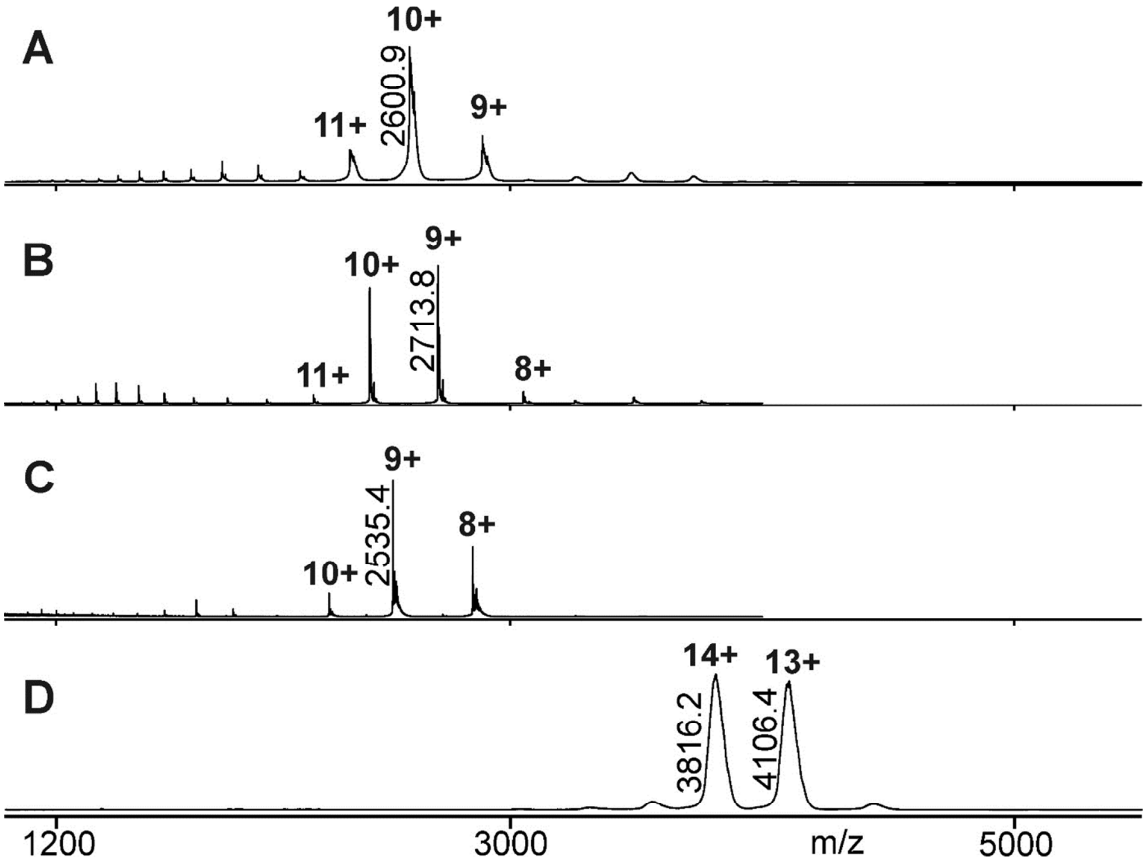


**Fig. S8** NanoESI mass spectra of protein G´ isoforms and IgG-Fc. A: protein G´e. B: protein G´f. **C:** protein G´g. **D:** IgG-Fc. Charge states and m/z values for selected ion signals of a respective ion series are given. Solvents: 200 mM $NH_4OAc$

**Collision induced protein-protein complex dissociation**

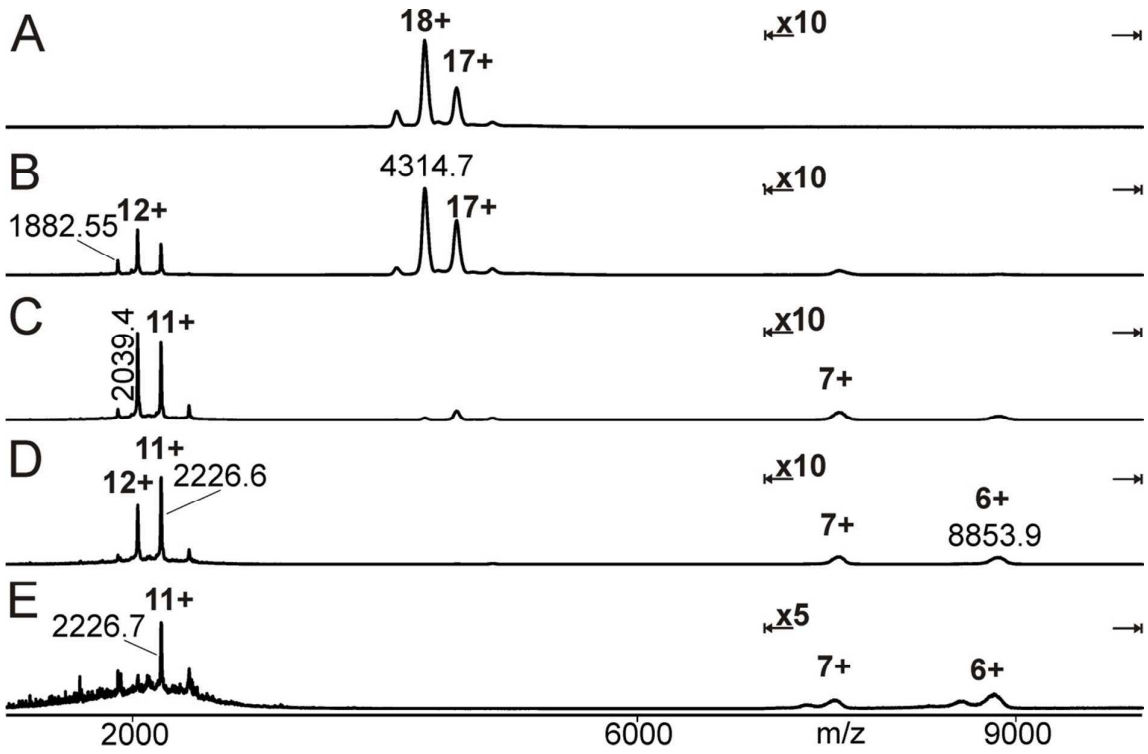


**Fig. S9** Collision induced dissociation of the ion mobility-separated IgG-Fc protein G'f complex. The complex was prepared and sprayed from 200 mM $NH_4OAc$ and measurement series with increasing transfer cell collision energies (TCE) were acquired as described. Example spectra recorded at (A) 70 V, (B) 120 V, (C) 150 V, (D) 170 V, and (E) 200 V are presented. Charge states and m/z values (from the apex of each peak in question) of released protein G'f product ions, IgG-Fc G'f precursor ions as, well as of retained IgG-Fc product ions are labeled. *Note*: At 200 V TCE signals of intact protein G'f are superimposed by backbone fragment ion signals

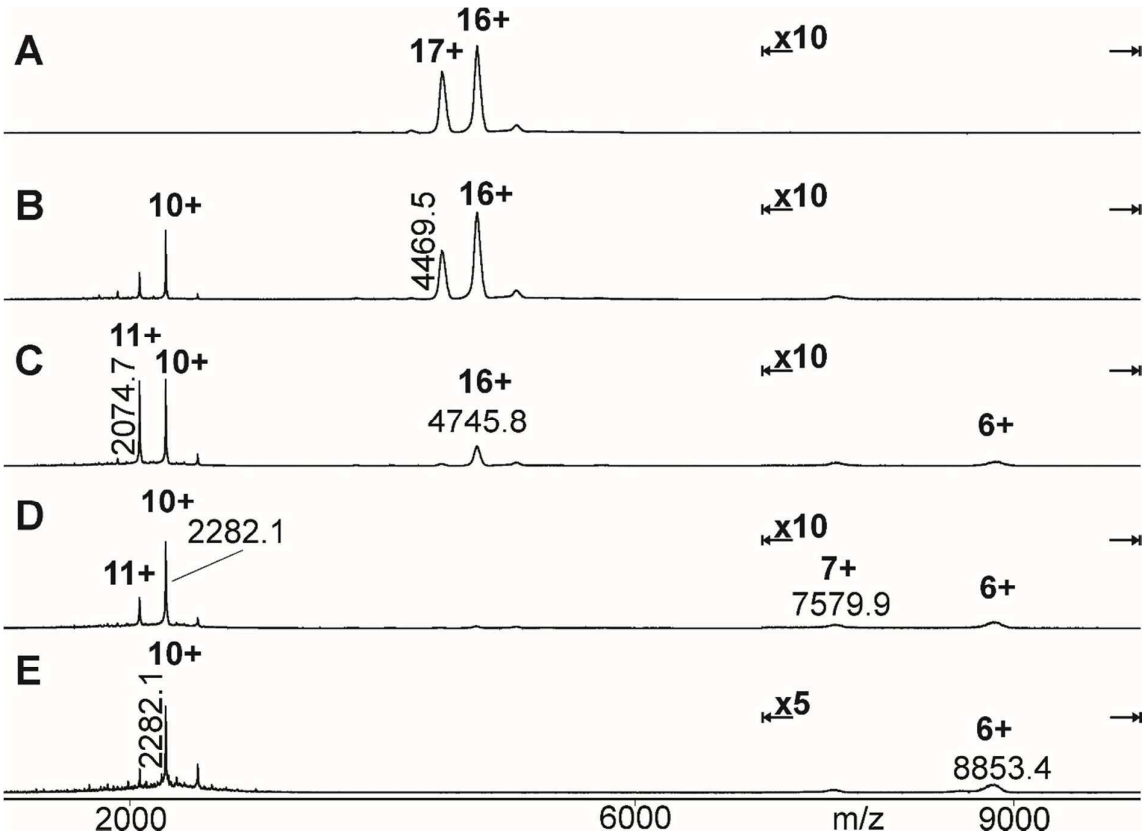


**Fig. S10** Collision induced dissociation of the ion mobility-separated IgG-Fc protein G'g complex. The complex was prepared and sprayed from 200 mM $NH_4OAc$ and measurement series with increasing transfer cell collision energies (TCE) were acquired as described. Example spectra recorded at (A) 70 V, (B) 120 V, (C) 150 V, (D) 170 V, and (E) 200 V are presented. Charge states and m/z values (from the apex of each peak in question) of released protein G'g product ions, IgG-Fc G'g precursor ions, as well as of retained IgG-Fc product ions are labeled. *Note*: At 200 V TCE signals of intact protein G'g are superimposed by backbone fragment ion signals

**In-solution $K_D$ value determinations**

The obtained in-solution data (see Materials and Methods) were stored in the SensMaster software. For evaluation of the sensograms the software FitMaster (Rev. 2.0; SAW Instruments, Bonn, Germany) coupled with Origin 8.1G (OriginLab corporation, Massachusetts, USA) was used. Fitting of the binding curves was done by applying the "1:1 Binding + Residue model" which assumes a permanently bound residue [45, 46]. Since the concentration of immobilised antibodies (IVIG) is in excess and remains almost unchanged during the interactions, the time course of phase changes that occurred during binding was fitted to a pseudo first order kinetics. The pseudo first order kinetic constant ($k_{obs}$) was determined for the different concentrations of analytes using equation (7), where *A* is the number of bound sites at any given time point (*t*) and $A_{eq}$ is the number of bound sites at equilibrium between absorption and desorption.

$$A(t) = A_{eq} * [1 - \exp\{-k_{obs} * t\}] \quad (7)$$

Next, $k_{obs(n)}$ values determined for different concentrations ($c_1$, $c_2$, … $c_n$) were subjected to linear regression described by equation (8).

$$k_{obs(n)} = k_{on} * c_n + k_{off} \quad (8)$$

A linear regression of concentration of analyte vs $k_{obs(n)}$ was subsequently used to obtain $k_{on}$ and $k_{off}$ values, where $k_{on}$ is the slope of the graph, $k_{off}$ is the intercept on the $k_{obs(n)}$ axis, and $c_n$ is the concentration of analytes. From these, $K_{D\,s}$ values were calculated according to equation (9).

$$K_{D\,s} = \frac{k_{off}}{k_{on}} \quad (9)$$

**Analytical and Bioanalytical Chemistry**

**Electronic Supplementary Material**

# Apparent activation energies of protein-protein complex dissociation in the gas phase determined by electrospray mass spectrometry

Yelena Yefremova, F. Teresa I. Melder, Bright D. Danquah, Kwabena F.M. Opuni, Cornelia Koy, Alexandra Ehrens, David Frommholz, Harald Illges, Knut Koelbel, Frank Sobott, Michael O. Glocker

## I) Theoretical background and method development



## II) Protein G´ • IgG-Fc

## I) Theoretical background and method development

### Basic considerations

Thermodynamic evaluation of gas-phase dissociation reactions of protein-protein complexes along well established laws for in-solution reactions, such as linear free energy relationships, is derived from considering the following facts and simplifications [17-21, 26, 27, 29, 30]:

1. Both, the protein-protein complex dissociation reaction itself (because of entropy gain of the products) and concomitant complex constituent unfolding reactions (due to lack of the hydrophobic effect which could drive refolding) are irreversible.
2. Within the energy "transition region" of the protein-protein complex dissociation reaction, the time required for recording single spectra is shorter than that which was needed for reaching complete unfolding/dissociation of protein-protein complexes.
3. Consequently, educt (protein-protein complex) and product (complex constituent) ion signals are simultaneously recorded in the corresponding mass spectra with elevated collision energies as opposed to the exclusive presence of educt ions in the "baseline region" as well as of only product ions in the maximum energy regime (disregarding potential fragmentation).

These considerations permit application of "Linear Free Energy relations" (LFE).

In-solution thermodynamic methods [10-16] were adapted to gas-phase experiments using the following conventions and definitions:

(1) $$\text{Normalized area under signal (norm. AUS)} = \left(f\,\frac{products}{educts}\right) * [\%] \quad (1)$$

(2) The charge contribution to the kinetic energy was accounted for by converting acceleration voltage ($V_{acc}$) into center of mass ($E_{com}$) energy:

$$E_{lab\ frame} = V_{acc} * z \quad (2)$$

$$E_{com} = \left(\frac{N}{m_p+N}\right) * E_{lab\ frame} \quad (3)$$

($N$ = mass of the neutral collision gas (here Ar, $M_r$ = 39.95); $m_p$ = mass of the protein-protein complex ion; z = charge)

(3) An "in-solution-like" LFE was applied to the "apparent equilibrium":

$$\Delta G_g^{\#} = -R * ln\left(\frac{100\% - norm.AUS}{norm.AUS}\right) = \Delta G_{m0g}^{\#} - \mathrm{n} * [E_{com}] \quad (4)$$

$R$ = gas constant, n = slope, m = mean of charge state, 0 = at $E_{com}$=0, g = gas phase. Principally, the absolute temperature, T, should be a factor in this equation, too, but since it cannot be determined with certainty, it was merged with the free enthalpy term. $\Delta G_{m0g}^{\#}$ must, therefore, be regarded as apparent.

(4) Extrapolation towards "zero activation", at $E_{com}$=0, yields the nominal stability (as opposed to observed parameters as threshold values) of complexes. However, because of the de facto irreversibility of the dissociation reaction (see above considerations), this value describes not a

thermodynamic (equilibrium) stability, but has to be regarded as being proportional to the activation energy ($E^{\#}_{A\,m0g}$): $\Delta G^{\#\,0}_{m0g} = E^{\#}_{A\,m0g}$ (5)

Plotting normalized AUS curves as functions of the respective lab frame or center-of-mass energies in order to obtain valid threshold energies has been accepted standard. But, Coulomb repulsion affects the unfolding and dissociation processes ("interface separation") of protein-protein complex ions in the gas phase. This dissociation process comprises two different aspects which need to be considered separately.

1) the charge impact on kinetic energy itself is conveniently corrected for by plotting the peak areas of complex ions and constituent ions, respectively, vs. lab frame or, as in our case, center-of-mass energies ($E_{com}$).
2) charge repulsion - as driving force for separation - is covered by our analysis by extrapolation towards $E_{com}$ = 0.

Further correction is not necessary, since we used the respective educt and product abundances (in the transition region) at energies that limit formation of charge repulsed products. Principally, this simplification is correct as long as the procedure is applied to each charge state separately. Of note, our experiments with streptavidin have shown that extrapolation lines from the different charge states are well represented by the line that is obtained by the data from the mean of the charge states.

Therefore, we determined the activation energy ($E^{\#}_{A\,m0g}$) at $E_{com}$=0 eV of protein-protein complexes by applying "Linear Free Energy relations" (LFE; cf. Figure S6B).

**Ion mobility separation of protein complex ions**

Our method was tested by dissociating the streptavidin tetramer (S4) with and without ion mobility selection of individual charge states using a Synapt mass spectrometer as described in the Materials and Methods section. A streptavidin tetramer (S4) stock solution was prepared by dissolving the commercial product (Carl-Roth, Karlsruhe, Germany, article no. 6073, lot no. 025218507; Mr (avg.): 56,116) in 50 mM $NH_4OAc$, pH 6.9 (final streptavidin (S4) concentration 1 mg/ml). Buffer exchange, using 50 mM $NH_4OAc$, pH 6.9 for all steps, protein concentration determination, and spectrum acquisition are described in the materials and methods section for IgG-Fc and protein G´-containing solutions.

Despite the fact that the 16+ streptavidin tetramer ion signal is located at the same m/z position as the 4+ streptavidin monomer ion signal, there is no risk of ambiguity in the assignment, since the latter appears at clearly different TCE / $E_{com}$ values as opposed to that of the first one. When dissociating the individual charge states 15+ and 14+ of the tetramer complex there is no overlap of tetramer with monomer ions.

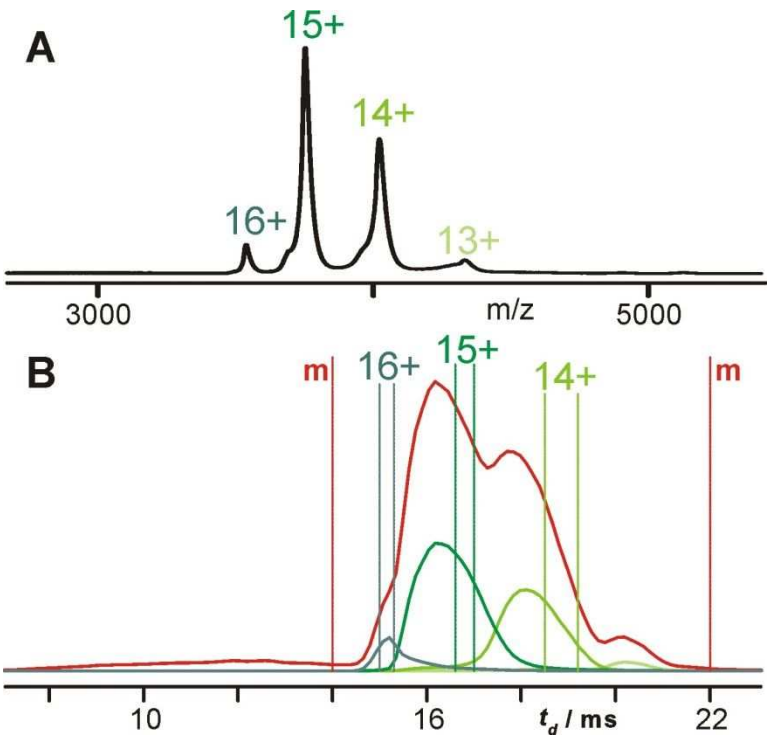


**Fig. S1** Ion mobility selection of tetrameric streptavidin ions. A: Precursor ion mass spectrum of the intact streptavidin tetramer recorded with 30 V acceleration voltage (TCE). Individual charge states are indicated above the respective peaks. B: Arrival time distributions corresponding to the complete spectrum (red) or to the individual charge states (same color code as in A). Drift time windows as used for abundance-weighted mean of charge states (m) and charge state-specific ion mobility selections (see Fig. S2-S5) are indicated by vertical ticked lines

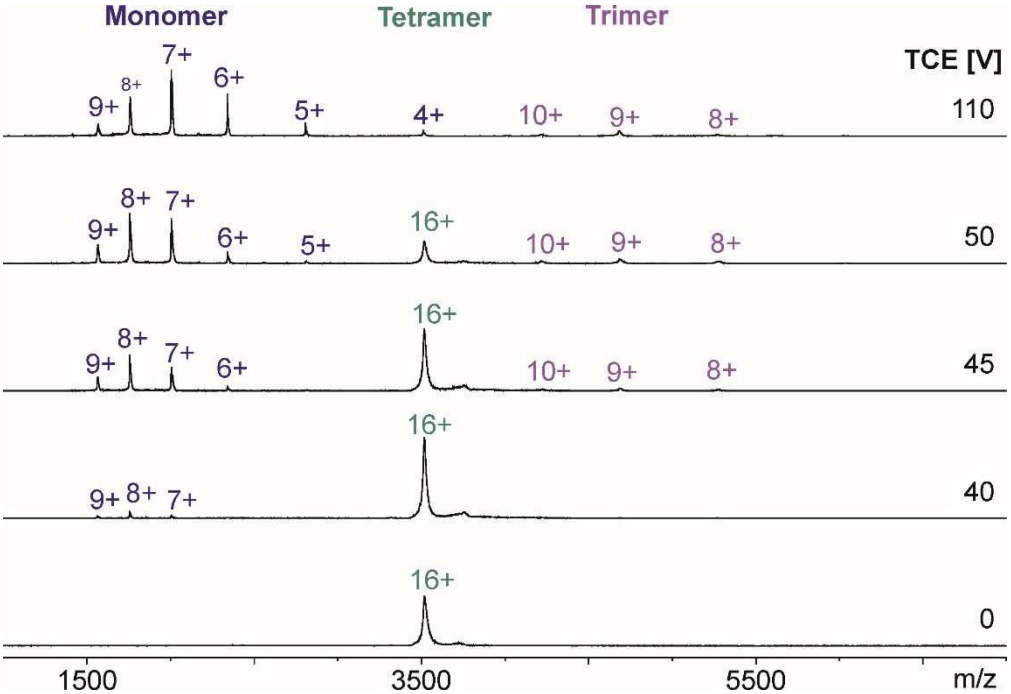


**Fig. S2** Collision induced dissociation of 16+ tetrameric streptavidin ion. NanoESI mass spectra of intact and dissociated streptavidin tetramers after ion mobility selection of the 16+ charge state and its subsequent collision induced dissociation by stepwise increasing transfer cell collision energies (TCE, from bottom to top)

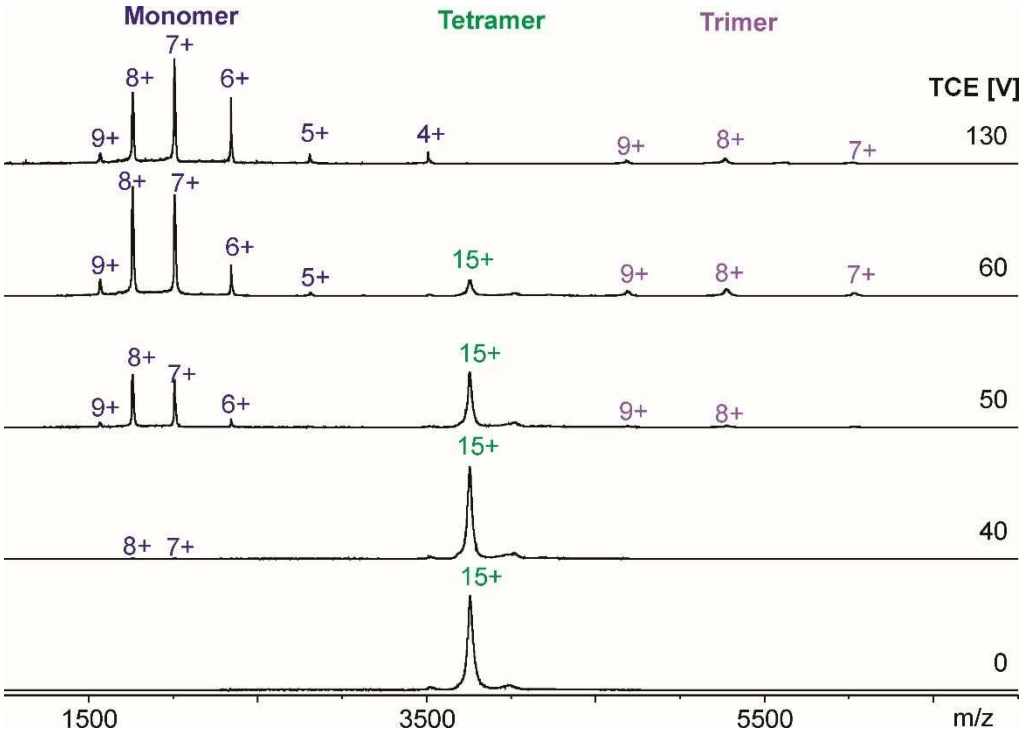


**Fig. S3** Collision induced dissociation of 15+ tetrameric streptavidin ion. NanoESI mass spectra of intact and dissociated streptavidin tetramers after ion mobility selection of the 15+ charge state and its subsequent collision induced dissociation by stepwise increasing transfer cell collision energies (TCE, from bottom to top)

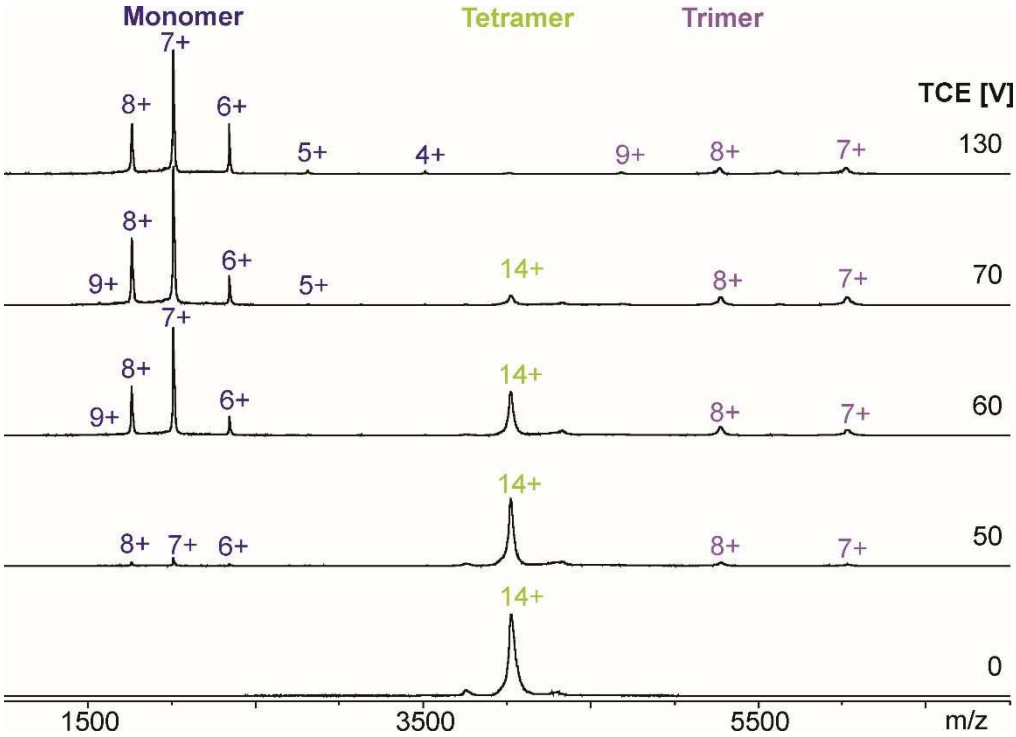


**Fig. S4** Collision induced dissociation of 14+ tetrameric streptavidin ion. NanoESI mass spectra of intact and dissociated streptavidin tetramers after ion mobility selection of the 14+ charge state and its subsequent collision induced dissociation by stepwise increasing transfer cell collision energies (TCE, from bottom to top)

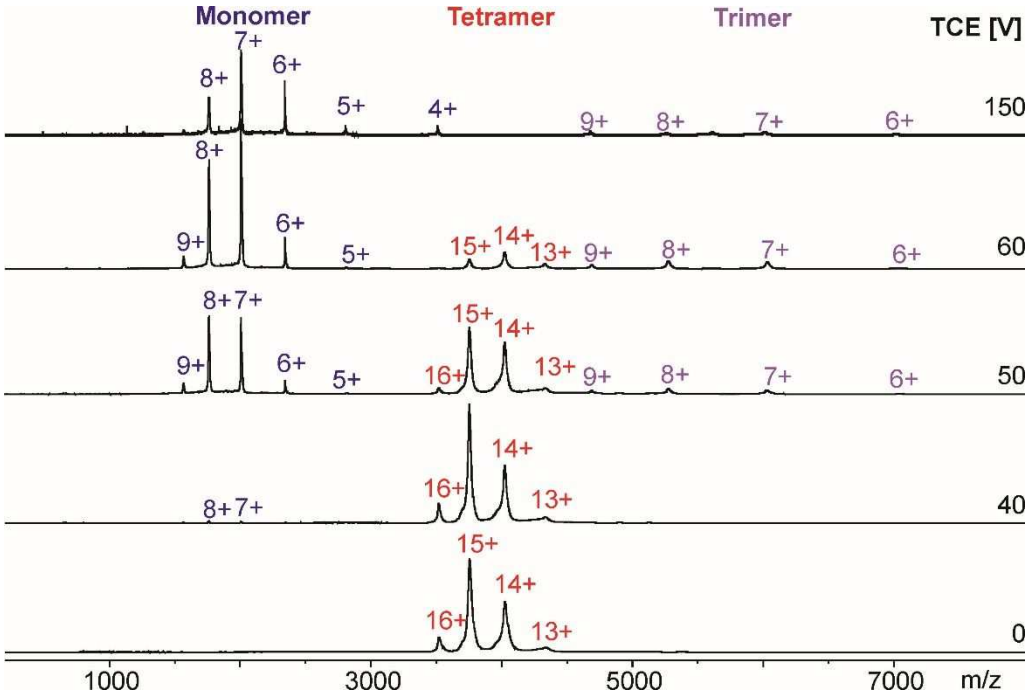


**Fig. S5** Collision induced dissociation of n+ tetrameric streptavidin ions. NanoESI mass spectra of intact and dissociated streptavidin tetramers after ion mobility selection of the abundance-weighted mean of charge states (m) and their subsequent collision induced dissociation by stepwise increasing transfer cell collision energies (TCE, from bottom to top)

**Evaluation of CID data of ion mobility-selected streptavidin complexes**

From Fig. S2-S5 the unaltered pattern of the highly charged monomeric product ions is apparent – regardless of precursor ion charge. Contrarily, the charge states of the respective precursor and dominant trimeric product ions correlate strictly. Since the classical asymmetric charge distribution pattern is adhered to, ion mobility selection can be conveniently used as surrogate of conventional MS/MS.

The unfolding/dissociation transitions of tetrameric streptavidin are steep (Fig. S6A), leaving only four to five data points for LFE evaluation. The potential error margin depends from either keeping or dropping the extreme points from analysis (Fig. S6B). Sufficient numbers of repetitions are therefore required. These, in turn, are more conveniently achieved for the complete sets of precursor ion peaks (m) than for each individual charge state. So, we widened the drift time window to encompass the complete tetrameric ensemble (+16 to +13, m; see Fig. S1) and measured dissociation of tetrameric streptavidin (S4) in triplicate (Fig. S5). An abundance-weighted mean of charge state (m) of 14.6+ was calculated using equation 6:

$$z = \sum z_n * \left(\frac{I_{z_n}}{\sum I}\right) \tag{6}$$

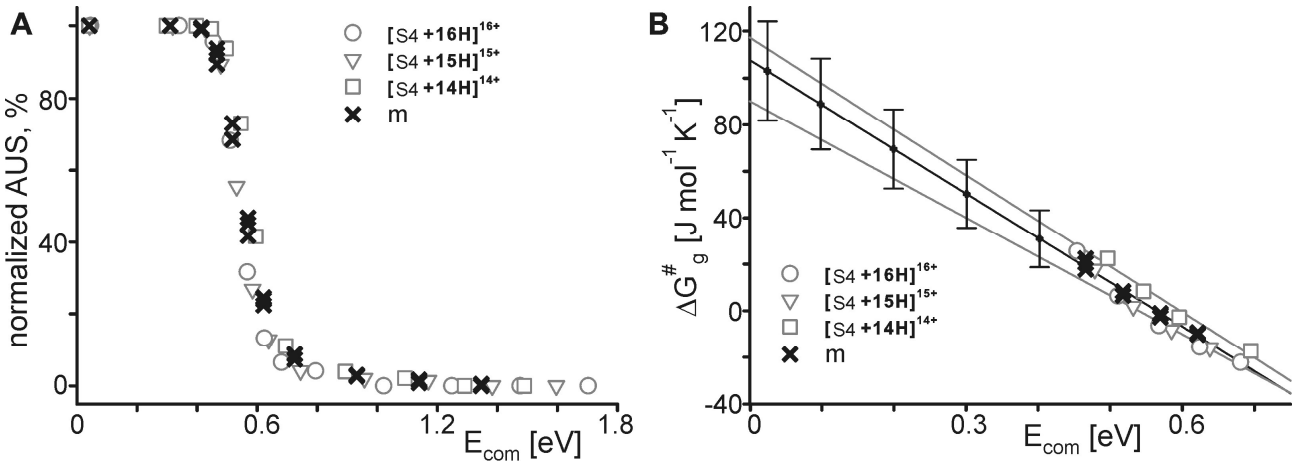


**Fig. S6** Evaluation of streptavidin complex gas-phase stabilities by LFE. A: Series of CID measurements using ion mobility-selected (see Fig. **S**1 for the respective drift time windows) tetrameric streptavidin (S4) were conducted and normalized areas under ion signals (normalized AUS) were determined as described. B: LFE evaluation was applied to the normalized AUS data. Selected data points were deliberately dropped from analysis to test for their effects on resulting deviations (maximum effects are within error bars).

Quite reasonably – as the mean of charge states inherently represents the most intense signal within the considered ensemble (+14 and +15 for S4) – LFE evaluation of these data closely resembles the corresponding results of the individual charge state-specific measurements. And, since the most intense native-MS peaks of a given protein are usually adjacent to each other, LFE evaluation of abundance-weighted mean of charge states will yield fairly representative $E^{\#}_{A\,m0g}$ values for the complete charge state ensemble of a given protein-protein complex.

## II) Protein G´ • IgG-Fc

**Amino acid sequences of protein G´ variants**

```
                FSN                                                  domain I
Protein G'e     GSSHHHHHHSSGLVPRGSHMASMTGGQQMGRDPNSSSVDKLAAALETYKLILNGKTLKGE
Protein G'g     ---------------------------------------------GTYKLILNGKTLKGE
Protein G'f     GSSHHHHHHSSGLVPRGSHMASMTGGQQMGRG-------------STYKLILAGKTLKGE

                                                   spacer 1
Protein G'e     TTTEAVDAATAEKVFKQYANDNGVDGEWTYDDATKTFTVTEKPEVIDASELTPAVTTYKL
Protein G'g     TTTEAVDAATAEKVFKQYANDNGVDGEWTYDDATKTFTVTEKPEVIDASELTPAVTTYKL
Protein G'f     TTTEAVDAATAEKVFKQYANDAGVDGEWTYDDATKTFTVTEKPEVIDASELTPAVTTYKL

                domain II                                           spacer 2
Protein G'e     VINGKTLKGETTTEAVDAATAEKVFKQYANDNGVDGEWTYDDATKTFTVTEKPEVIDASE
Protein G'g     VINGKTLKGETTTEAVDAATAEKVFKQYANDNGVDGEWTYDDATKTFTVTEKPEVIDASE
Protein G'f     ILAGKTLKGETTTEAVDAATAEKVFKQYANDAGVDGEWTYDDATKTFTVTEKPEVIDASE

                     domain III
Protein G'e     LTPAVTTYKLVINGKTLKGETTTKAVDAETAEKAFKQYANDNGVDGVWTYDDATKTFTVT
Protein G'g     LTPAVTTYKLVINGKTLKGETTTKAVDAETAEKAFKQYANDNGVDGVWTYDDATKTFTVT
Protein G'f     LTPAVTTYKLILAGKTLKGETTTEAVDAATAEKVFKQYANDAGVDGEWTYDDATKTFTVT

                        FSC
Protein G'e     E-------------
Protein G'g     EKIAAALEHHHHHH
Protein G'f     E-------------
```

**Fig. S7** Amino acid alignment of the three protein G’ variants. The amino acid sequences of proteins G’e, G’g and G’f (from top to bottom in each single panel) are aligned with the N- and C-termini shown in italics. Kinked arrows encompass the complete IgG binding domains, whereas boxes indicate regions known to be actually involved in IgG binding. Distinct domains and linkers of the proteins are labeled individually above the sequences: the N- and C-terminal flanking sequences (FSN and FSC, respectively), the three IgG binding domains (I-III) and the spacer regions in between. Residues, the exchanges of which distinguish protein G’f from the other two, are underlined

**Data on individual complex constituents**

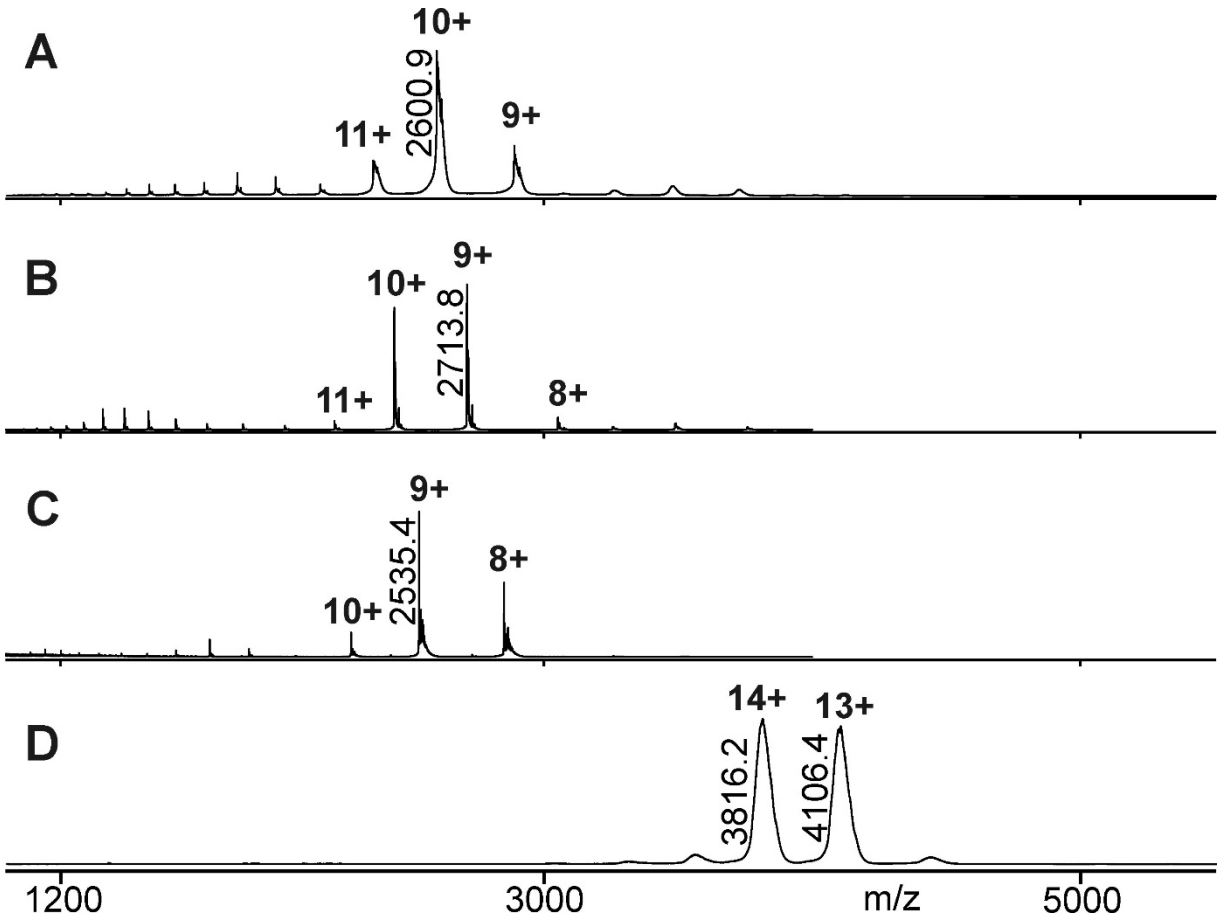


**Fig. S8** NanoESI mass spectra of protein G´ isoforms and IgG-Fc. A: protein G´e. B: protein G´f. **C:** protein G´g. **D:** IgG-Fc. Charge states and m/z values for selected ion signals of a respective ion series are given. Solvents: 200 mM $NH_4OAc$

**Collision induced protein-protein complex dissociation**

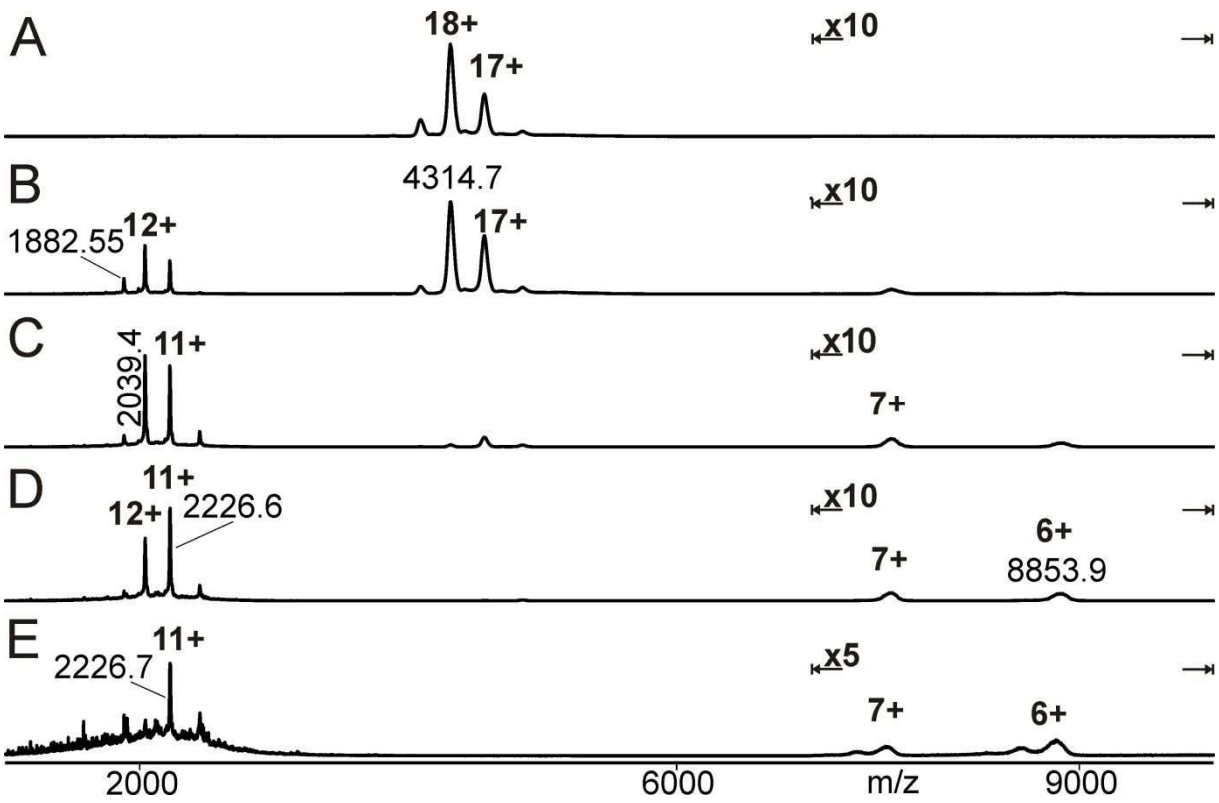


**Fig. S9** Collision induced dissociation of the ion mobility-separated IgG-Fc protein G'f complex. The complex was prepared and sprayed from 200 mM $NH_4OAc$ and measurement series with increasing transfer cell collision energies (TCE) were acquired as described. Example spectra recorded at (A) 70 V, (B) 120 V, (C) 150 V, (D) 170 V, and (E) 200 V are presented. Charge states and m/z values (from the apex of each peak in question) of released protein G'f product ions, IgG-Fc G'f precursor ions as, well as of retained IgG-Fc product ions are labeled. *Note*: At 200 V TCE signals of intact protein G'f are superimposed by backbone fragment ion signals

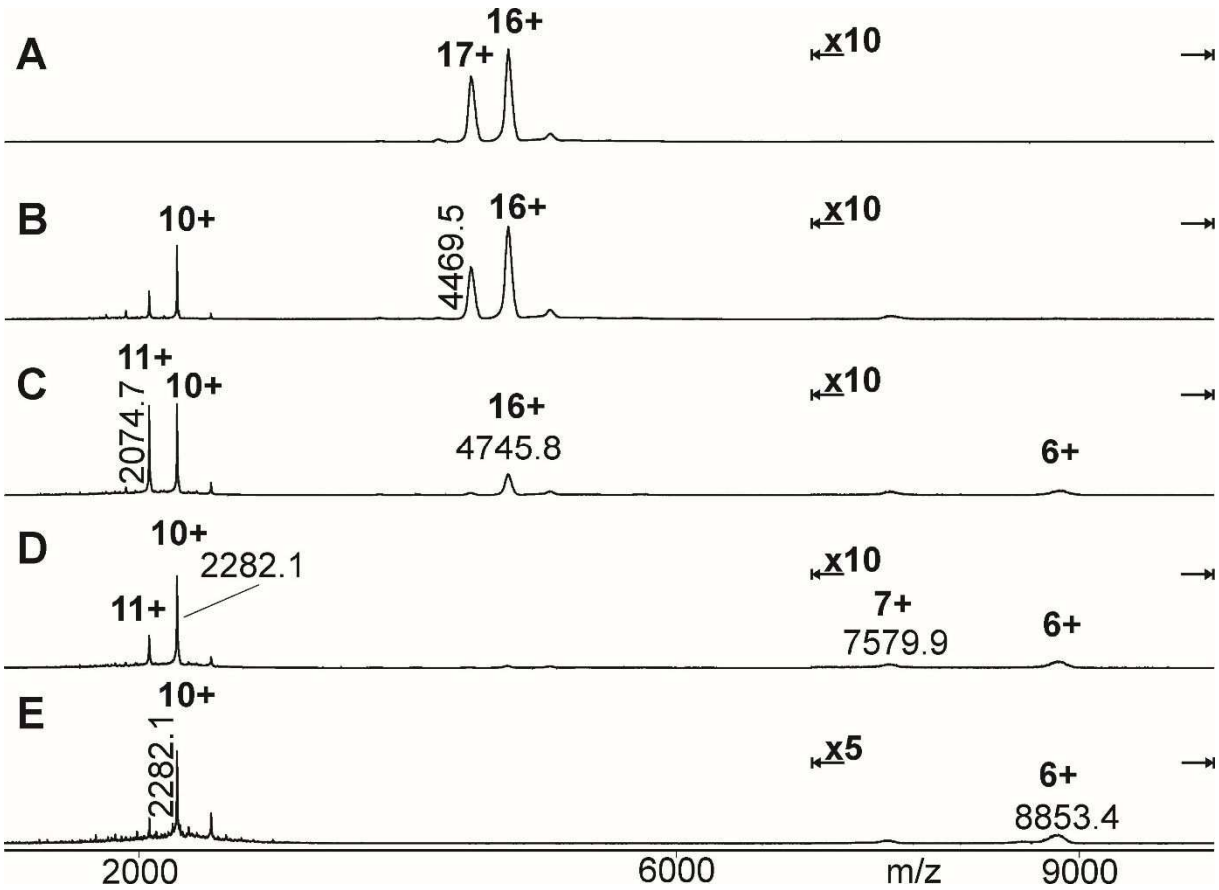


**Fig. S10** Collision induced dissociation of the ion mobility-separated IgG-Fc protein G'g complex. The complex was prepared and sprayed from 200 mM $NH_4OAc$ and measurement series with increasing transfer cell collision energies (TCE) were acquired as described. Example spectra recorded at (A) 70 V, (B) 120 V, (C) 150 V, (D) 170 V, and (E) 200 V are presented. Charge states and m/z values (from the apex of each peak in question) of released protein G'g product ions, IgG-Fc G'g precursor ions, as well as of retained IgG-Fc product ions are labeled. *Note*: At 200 V TCE signals of intact protein G'g are superimposed by backbone fragment ion signals

**In-solution $K_D$ value determinations**

The obtained in-solution data (see Materials and Methods) were stored in the SensMaster software. For evaluation of the sensograms the software FitMaster (Rev. 2.0; SAW Instruments, Bonn, Germany) coupled with Origin 8.1G (OriginLab corporation, Massachusetts, USA) was used. Fitting of the binding curves was done by applying the "1:1 Binding + Residue model" which assumes a permanently bound residue [45, 46]. Since the concentration of immobilised antibodies (IVIG) is in excess and remains almost unchanged during the interactions, the time course of phase changes that occurred during binding was fitted to a pseudo first order kinetics. The pseudo first order kinetic constant ($k_{obs}$) was determined for the different concentrations of analytes using equation (7), where *A* is the number of bound sites at any given time point (*t*) and $A_{eq}$ is the number of bound sites at equilibrium between absorption and desorption.

$$A(t) = A_{eq} * [1 - \exp\{-k_{obs} * t\}] \quad (7)$$

Next, $k_{obs(n)}$ values determined for different concentrations ($c_1$, $c_2$, … $c_n$) were subjected to linear regression described by equation (8).

$$k_{obs(n)} = k_{on} * c_n + k_{off} \quad (8)$$

A linear regression of concentration of analyte vs $k_{obs(n)}$ was subsequently used to obtain $k_{on}$ and $k_{off}$ values, where $k_{on}$ is the slope of the graph, $k_{off}$ is the intercept on the $k_{obs(n)}$ axis, and $c_n$ is the concentration of analytes. From these, $K_{D\,s}$ values were calculated according to equation (9).

$$K_{D\,s} = \frac{k_{off}}{k_{on}} \quad (9)$$